







Phosphatidic acid modulates MPK3- and MPK6-mediated hypoxia signaling in Arabidopsis

Ying Zhou,¹ De-Mian Zhou,¹ Wei-Wei Yu,¹ Li-Li Shi,¹ Yi Zhang ,¹ Yong-Xia Lai,¹ Li-Ping Huang,¹ Hua Qi ,^{2,3} Qin-Fang Chen ,¹ Nan Yao ,¹ Jian-Feng Li ,¹ Li-Juan Xie^{2,3,*†} and Shi Xiao ^{1,3,*†}

- 1 State Key Laboratory of Biocontrol, Guangdong Provincial Key Laboratory of Plant Resources, School of Life Sciences, Sun Yat-sen University, Guangzhou 510275, China
- 2 Provincial Key Laboratory of Agricultural & Rural Pollution Abatement and Environmental Safety, College of Natural Resources and Environment, South China Agricultural University, Guangzhou 510642, China
- 3 Guangdong Laboratory for Lingnan Modern Agriculture, Guangzhou 510642, China

*Authors for correspondence: xiaoshi3@mail.sysu.edu.cn (S.X.) and xielijuan@scau.edu.cn (L.J.X.)

†Senior authors

S.X. and L.J.X. designed the research. Z.Y., L.J.X., D.M.Z., W.W.Y., L.L.S., Y.Z., Y.X.L., W.J.T., H.Q., and Q.F.C. carried out the experiments. S.X., L.J.X., and Y.Z. analyzed the data and wrote the manuscript.

The author responsible for distribution of materials integral to the findings presented in this article in accordance with the policy described in the Instructions for Authors (<https://academic.oup.com/plcell>) is: Shi Xiao (xiaoshi3@mail.sysu.edu.cn).

Abstract

Phosphatidic acid (PA) is an important lipid essential for several aspects of plant development and biotic and abiotic stress responses. We previously suggested that submergence induces PA accumulation in *Arabidopsis thaliana*; however, the molecular mechanism underlying PA-mediated regulation of submergence-induced hypoxia signaling remains unknown. Here, we showed that in Arabidopsis, loss of the phospholipase D (PLD) proteins PLD α 1 and PLD δ leads to hypersensitivity to hypoxia, but increased tolerance to submergence. This enhanced tolerance is likely due to improvement of PA-mediated membrane integrity. PA bound to the mitogen-activated protein kinase 3 (MPK3) and MPK6 in vitro and contributed to hypoxia-induced phosphorylation of MPK3 and MPK6 in vivo. Moreover, *mpk3* and *mpk6* mutants were more sensitive to hypoxia and submergence stress compared with wild type, and fully suppressed the submergence-tolerant phenotypes of *pld α 1* and *pld δ* mutants. MPK3 and MPK6 interacted with and phosphorylated RELATED TO AP2.12, a master transcription factor in the hypoxia signaling pathway, and modulated its activity. In addition, MPK3 and MPK6 formed a regulatory feedback loop with PLD α 1 and/or PLD δ to regulate PLD stability and submergence-induced PA production. Thus, our findings demonstrate that PA modulates plant tolerance to submergence via both membrane integrity and MPK3/6-mediated hypoxia signaling in Arabidopsis.

Introduction

Terrestrial plants frequently experience low oxygen (O₂) tension (hypoxia) caused by root waterlogging or complete submergence. Hypoxia leads to an energy crisis resulting from the lack of O₂ and the accumulation of toxic metabolites, which impair plant growth and development. In response to

hypoxia, plants can alter their architecture to attempt to rise above the water line; in addition, submerged plants undergo reprogramming of gene expression and cellular metabolism to improve their survival of hypoxia stress (Bailey-Serres and Voesenek, 2008; Xie et al., 2021). Increasing evidence indicates that multiple regulatory components,

including plant hormones, transcription factors, and protein kinases, are involved in plant responses to hypoxic stress (Sasidharan et al., 2018; Schmidt et al., 2018).

Sensing O_2 levels is important for the response to hypoxia. Homeostatic oxygen sensing is tightly regulated by group VII ethylene response factors (ERFs-VII), including RELATED TO APETALA2.12 (RAP2.12), RAP2.2, RAP2.3, HYPOXIA-RESPONSIVE ERF1 (HRE1), and HRE2, via the N-end rule proteolysis pathway (Gibbs et al., 2011; Licausi et al., 2011; Sasidharan and Mustroph, 2011). RAP2.12 associates with the plasma membrane through its physical interaction with the membrane-anchored proteins ACYL-CoA-BINDING PROTEIN1 (ACBP1) and ACBP2 under normal air supply. Upon hypoxic stress, RAP2.12 is released from the plasma membrane and translocates to the nucleus, where it activates the transcription of downstream hypoxia-responsive genes (Gibbs et al., 2011; Licausi et al., 2011; Sasidharan and Mustroph, 2011). More recently, two independent studies have suggested that unsaturated long-chain acyl-CoAs likely act as signaling lipids that promote responses to hypoxia by modulating the dynamics of the ACBP1/2–ERF-VII complex (Schmidt et al., 2018; Zhou et al., 2020).

In plant cells, the plasma membrane is the site of stress perception and signal transduction in response to various abiotic and biotic stresses and lipid signaling is a key for the response to these stresses. For example, diverse developmental and environmental cues activate phospholipase D (PLD), which cleaves membrane phospholipids to generate phosphatidic acid (PA) and a free head group. PLDs are activated in response to abscisic acid (ABA; Zhang et al., 2004; Mishra et al., 2006; Zhang et al., 2009), high salt (Katagiri et al., 2001; Bargmann et al., 2009a; Yu et al., 2010), freezing temperatures (Li et al., 2004; Zhang et al., 2013), drought (Hong et al., 2010), phosphate starvation (Cruz-Ramírez et al., 2006), wounding (Bargmann et al., 2009b), and pathogen infection (Pinosa et al., 2013; Zhao et al., 2013; Hyodo et al., 2015). The induction of PLD activity, as well as the generation and abundance of PA under these conditions, indicates a crucial function for PLD and PA in abiotic and biotic stress tolerance in plants. Our findings demonstrated that submergence leads to substantial accumulation of PA (Xie et al., 2015a), suggesting that PA may have an important role in plant responses to hypoxic stress. However, the molecular mechanism by which plant PLDs function in response to hypoxia is still unknown.

The Arabidopsis (*Arabidopsis thaliana*) PLD family comprises 12 members, which are grouped into six types: PLD α , β , γ , δ , ϵ , and ζ (Wang, 2005). The PLD α 1 and PLD δ isoforms are the two most abundant PLDs and are redundantly required for resistance to high salinity and hyperosmotic stress (Bargmann et al., 2009a). In contrast, these isoforms have opposite roles during responses to cold stress (Welti et al., 2002; Li et al., 2004), indicating that each PLD has a distinct function in stress responses. Moreover, PLD α 1 and PLD δ interact with a number of proteins, thereby playing important roles in several cellular processes (Uraji et al.,

2012). In addition, PA itself binds to the Arabidopsis NADPH oxidases respiratory burst oxidase homolog D (RbohD) and RbohF, triggering NADPH oxidase activity in response to the ABA-mediated production of reactive O_2 species (ROS; Zhang et al., 2009). PA also interacts with and stimulates mitogen-activated protein kinase 6 (MPK6), which in turn promotes the phosphorylation of the Na^+ / H^+ antiporter SALT OVERLY SENSITIVE1 (SOS1), thus conferring salinity tolerance in Arabidopsis (Yu et al., 2010).

Arabidopsis mitogen-activated protein kinase (MAPK or MPK) cascades convert the perception of environmental and developmental cues into cellular responses, and typically involve three protein kinases: a MAPK kinase kinase, a MAPK kinase (MAPKK), and a MAPK. Signals are transduced via a phosphorylation cascade from upstream kinases to their downstream targets. Several well-studied plant MAPKs, including MPK3, MPK6, and their orthologs, serve as key regulators in response to a wide range of physiological processes, such as development, innate immunity, and phytohormone signaling (Colcombet and Hirt, 2008; Rodriguez et al., 2010).

Increasing evidence suggests that MPK3 and MPK6 play a positive role in plant responses to hypoxic stress (Chang et al., 2012; Cho et al., 2016; Singh and Sinha, 2016). In particular, MPK3, MPK4, and MPK6 are activated by O_2 deprivation, and transgenic Arabidopsis lines overexpressing MPK6 showed enhanced tolerance to anoxia (Chang et al., 2012). Moreover, rice (*Oryza sativa*) MPK3 interacts with and phosphorylates the ERF-VII transcription factor SUBMERGENCE 1A (SUB1A) to form a positive feedback loop, thus contributing to submergence tolerance (Singh and Sinha, 2016). However, to date the upstream regulators controlling the MPK3/6–ERF-VII module remain obscure. In this study, we discovered that submergence triggers PA accumulation through the activation of PLD α 1 and PLD δ . Subsequently, PA activates MPK3 and MPK6 to phosphorylate RAP2.12, which is likely a key step in the initiation of hypoxia sensing and responses in Arabidopsis.

Results

Submergence induces PLD α 1- and PLD δ -mediated PA production

We previously found that submergence causes a significant increase in PA contents, but also a decrease in phosphatidylcholine (PC) and phosphatidylethanolamine (PE) contents (Xie et al., 2015a). To investigate PA dynamics in response to submergence, we analyzed the phospholipid profiles in 4-week-old wild-type (WT) Arabidopsis rosettes before and after submergence for 10 min and 48 h, followed by recovery for 10 min and 1 h, through electrospray ionization–tandem mass spectrometry. As shown in Figure 1A, submergence induced a rapid accumulation of PA, with a maximum 2.4-fold increase occurring 10 min after submergence compared to control rosettes.

In contrast, total PC and PE levels showed a significant decrease in response to submergence for 48 h (Figure 1A).

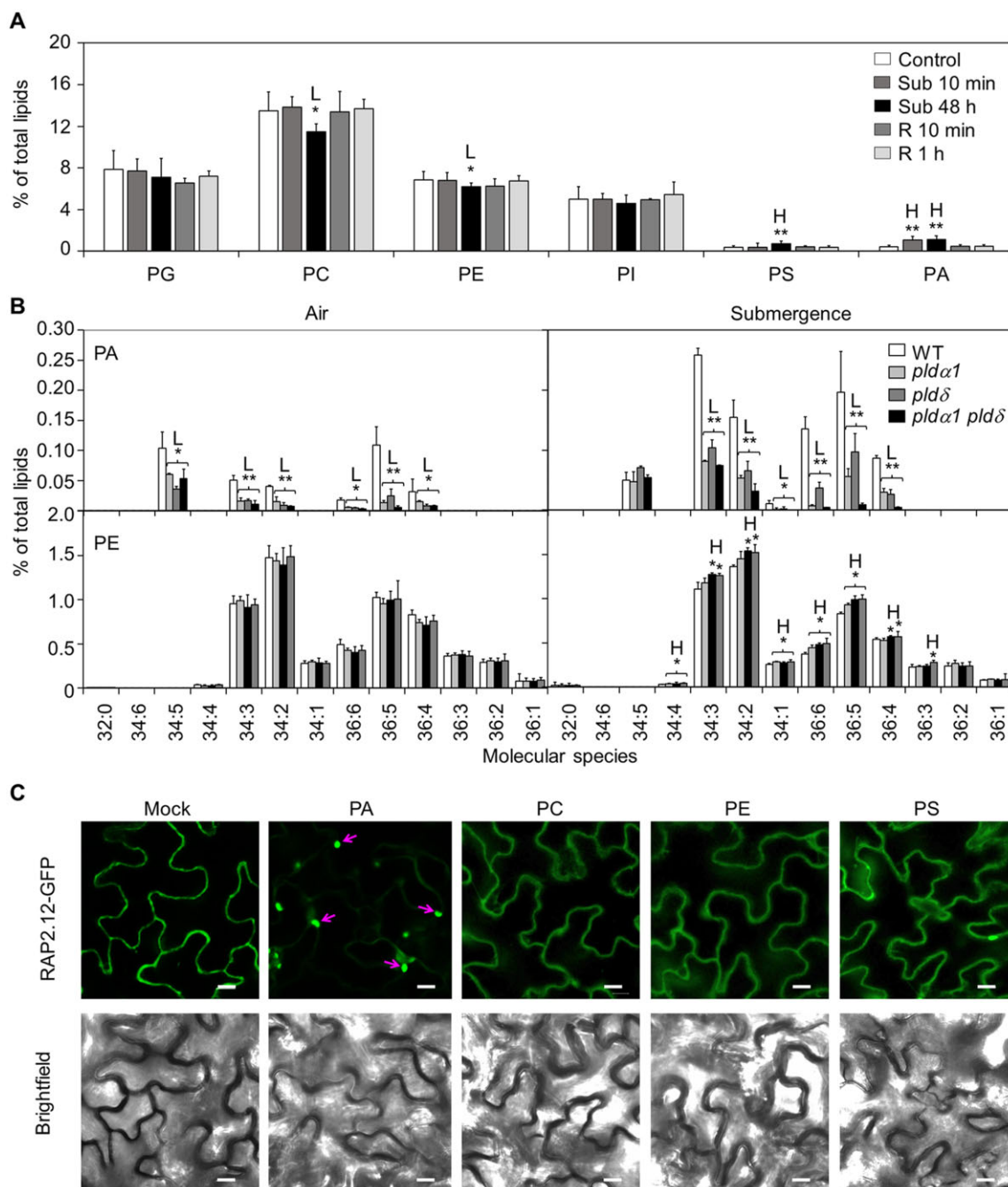


Figure 1 Submergence induces PLD α 1- and PLD δ -derived PA accumulation, which triggers the nuclear localization of RAP2.12. **A**, Amounts of membrane lipids (PG, PC, PE, PI, PS, and PA) in the rosettes of 4-week-old WT Col-0 plants under light submergence treatment (Sub) and after recovery (R) for the indicated times. **B**, Various PA and PE species in the rosettes of 4-week-old WT, *pld α 1*, *pld δ* , and *pld α 1 pld δ* plants before light submergence treatment (air) and after 2 days of submergence treatment (submergence). **C**, Exogenous application of PA, but not PC, PE, or PS, induces the translocation of RAP2.12-GFP from the plasma membrane to the nucleus. Detached leaves of 3-week-old RAP2.12-GFP transgenic plants were treated with 50- μ M liposomes prepared from PA, PC, PE, or PS (natural lipid mixtures purified from soy, Avanti Polar Lipids) for 3 h. Leaves similarly treated with dilution buffer were set as mock controls (Mock). The GFP fluorescence was detected by confocal microscopy. Red arrows indicate nuclear signal induced by PA application. Bars, 20 μ m. All experiments were performed on three biological replicates with similar results. Values represent means \pm SD ($n = 4$) of four independent technical replicates, and each replicate was collected from the rosettes of at least seven plants. Asterisks with “H” or “L” indicate significantly higher or lower levels than in control plants (A) or in WT (B) at each time point (* $P < 0.05$, ** $P < 0.01$ by Student’s t test).

Phosphatidylserine (PS) also accumulated to significantly higher levels upon submergence for 48 h (Figure 1A), consistent with previous findings (Xie et al., 2015a). Finally, all

submergence-induced changes in PA, PC, PE, and PS contents returned to normal levels upon reoxygenation for 10 min and 1 h (Figure 1A).

Table 1 Lipid profiling (% of total lipids) of 4-week-old leaves of WT, *pldα1*, *pldδ*, and *pldα1 pldδ* plants before and after 48-h submergence

Lipid Class	Air				Submergence					
	WT		<i>pldα1</i>		WT		<i>pldα1</i>		<i>pldα1 pldδ</i>	
	WT	<i>pldα1</i>	<i>pldδ</i>	<i>pldα1 pldδ</i>	WT	<i>pldα1</i>	<i>pldδ</i>	<i>pldα1 pldδ</i>		
DGDG	22.80 ± 1.12	21.49 ± 0.28	21.61 ± 1.31	20.82 ± 1.59	23.69 ± 0.33	22.69 ± 1.61	22.90 ± 1.01	24.32 ± 0.52		
Monogalactosyldiacylglycerol	43.43 ± 2.04	43.27 ± 1.61	44.43 ± 0.50	43.83 ± 2.10	42.61 ± 2.98	43.56 ± 2.38	44.54 ± 0.07	44.38 ± 0.48		
PG	8.49 ± 0.62	9.70 ± 0.19	8.55 ± 1.56	9.18 ± 2.64	8.36 ± 1.92	8.70 ± 2.17	8.66 ± 0.60	9.07 ± 0.59		
PC	12.56 ± 0.67	13.23 ± 0.50	11.48 ± 1.01	12.58 ± 0.52	10.85 ± 0.66^a	10.27 ± 0.01	10.29 ± 0.16	10.40 ± 0.18		
PE	6.45 ± 0.40	6.26 ± 0.06	5.92 ± 0.89	6.35 ± 0.34	5.79 ± 0.01^a	6.36 ± 0.04^{a,b}	6.49 ± 0.21^{a,b}	6.79 ± 0.11^{a,b}		
PI	4.66 ± 0.39	5.24 ± 1.50	4.82 ± 0.12	4.67 ± 0.35	5.44 ± 2.04	6.03 ± 1.76	5.16 ± 0.99	5.66 ± 0.72		
PS	0.38 ± 0.020	0.34 ± 0.040	0.30 ± 0.062	0.32 ± 0.024	0.50 ± 0.070^a	0.56 ± 0.107	0.43 ± 0.065	0.50 ± 0.077		
PA	0.44 ± 0.048	0.14 ± 0.030^a	0.12 ± 0.023^a	0.09 ± 0.023^a	0.97 ± 0.114^a	0.27 ± 0.022^{a,b}	0.39 ± 0.095^{a,b}	0.16 ± 0.037^{a,b}		
LysoPG	0.024 ± 0.001	0.023 ± 0.001	0.022 ± 0.001	0.023 ± 0.005	0.026 ± 0.001	0.021 ± 0.004	0.022 ± 0.001^b	0.026 ± 0.001		
LysoPC	0.021 ± 0.001	0.016 ± 0.002^a	0.018 ± 0.002	0.020 ± 0.002	0.018 ± 0.001	0.018 ± 0.001	0.015 ± 0.003	0.018 ± 0.001		
LysoPE	0.026 ± 0.003	0.018 ± 0.001^a	0.021 ± 0.002	0.020 ± 0.001^a	0.025 ± 0.001	0.021 ± 0.001^b	0.023 ± 0.001	0.026 ± 0.002		

Values are means ± SD (n = 4). Significant differences in the samples to that of controls are in bold.

^aValues were compared to WT 0 h.

^bValues were compared to WT submergence for 48 h

*P < 0.05;

**P < 0.01 by Student's t test.

Interestingly, we noticed that the increase in PA after submergence for 10 min was not accompanied by a reduction in PC or PE levels (Figure 1A), indicating that the short-term (10 min) and long-term (48 h) accumulation of PA may be produced through distinct routes in planta. In Arabidopsis, PLD-mediated hydrolysis of phospholipids and DIACYLGLYCEROL (DAG) KINASE (DGK)-catalyzed phosphorylation of DAG are two major routes for PA production (Wang et al., 2006; Arisz et al., 2009, 2013; Li-Beisson et al., 2013; Wang et al., 2014; Li et al., 2019). The submergence-induced expression of PLDs and DGKs appeared to be differentially regulated, as determined by RT-quantitative PCR (qPCR). Indeed, relative transcript levels of *DGK1* and *DGK5* were upregulated at 10 min after submergence, compared to the later induction of *PLDα1* and *PLDδ* expression upon submergence for 3 and 48 h (Supplemental Figure S1).

To verify whether PLDs contribute to PA accumulation during the plant response to submergence, we identified T-DNA insertional mutants in the two predominant Arabidopsis PLD genes, *PLDα1* and *PLDδ* (Supplemental Figure S2). Molecular characterization indicated that all mutants are likely null mutants for the corresponding PLD genes, as we failed to detect transcripts (Supplemental Figure S2). We also generated the corresponding *pldα1 pldδ* double mutant by genetic crossing for functional analysis. Lipid profiling showed that the relative PA levels are significantly lower in the *pldα1*, *pldδ*, and *pldα1 pldδ* mutants compared to those of the WT under normoxic conditions (Table 1), confirming previous findings (Bargmann et al., 2009b). After submergence for 48 h, PA levels further declined in all three mutants, with a reduction of 72%, 60%, and 84% in the *pldα1*, *pldδ*, and *pldα1 pldδ* mutants, respectively, compared to the submerged WT control (Table 1). In particular, the levels of 34:3-, 34:2-, 36:6-, 36:5-, and 36:4-PA species were much lower in the three *pld* mutants under both normoxic and submergence conditions relative to the WT (Figure 1B). In contrast, the total levels and different molecular species of PE were significantly higher in the *pldα1*, *pldδ*, and *pldα1 pldδ* mutants than in the WT (Table 1 and Figure 1B), suggesting that PE is a primary substrate for PLDα1 and PLDδ to produce PA in response to submergence. Taken together, these findings indicate that PLDα1 and PLDδ may contribute to submergence-induced accumulation of PA in Arabidopsis.

To further explore the potential link between PA and hypoxia signaling, we exposed detached leaves of 3-week-old *RAP2.12-GREEN FLUORESCENT PROTEIN* (GFP) transgenic plants expressing *RAP2.12-GFP* to 50 μM of liposomes consisting of PA, PC, PE, or PS, for 3 h, and determined the localization of the GFP fusion proteins by confocal microscopy. Compared to mock controls, application of PA, but not PC, PE, or PS, resulted in the translocation of *RAP2.12-GFP* from the plasma membrane to the nucleus (Figure 1C). Thus, our results suggest that PLDα1- and PLDδ-mediated release of PA upon submergence may play a crucial role in regulating hypoxia responses in Arabidopsis.

The *pldα1* and *pldδ* mutants show distinct phenotypes in response to hypoxia and submergence

To delineate the functions of PLD α 1 and PLD δ in plant responses to hypoxic stress, we performed phenotypic analyses of *pldα1*, *pldδ*, and *pldα1 pldδ* mutants exposed to hypoxia and submergence. We first analyzed the phenotypes of *pldα1*, *pldδ*, and *pldα1 pldδ* mutants subjected to hypoxic stress using seed germination and seedling damage assays. The *pldα1*, *pldδ*, and *pldα1 pldδ* seeds germinated on Murashige and Skoog (MS) solid medium for 10 days (Figure 2A) or 6-day-old seedlings transferred to MS medium for 5 days (Figure 2C) showed few morphological differences relative to WT seedlings when maintained under normoxic conditions (21% O₂). In contrast, when O₂ levels were dropped to 3%, the percentage of seedlings with green cotyledons was significantly lower in the *pldα1*, *pldδ*, and *pldα1 pldδ* mutants relative to WT (Figure 2, A and B). Indeed, hypoxia-induced leaf damage was more severe in the *pldα1*, *pldδ*, and *pldα1 pldδ* mutants than in WT seedlings (Figure 2C), as evidenced by the significantly lower survival rates seen for the *pld* mutants upon reoxygenation (Figure 2D). Furthermore, after submergence for 10 days, followed by a 3-day recovery, all 4-week-old *pld* mutant plants fared better than WT plants (Figure 2E). We validated the enhanced tolerance to submergence exhibited by *pldα1*, *pldδ*, and *pldα1 pldδ* mutants by measuring their dry weights upon submergence, followed by a 7-day recovery (Figure 2F).

In response to cold-induced dehydration stress, PA levels decrease, resulting in enhanced freezing tolerance, likely by preventing the PA-mediated formation of a destabilized hexagonal II (H_{II})-type lipid phase (Tan et al., 2018). We hypothesized that the same mechanism may contribute to the increased submergence tolerance of *pldα1*, *pldδ*, and *pldα1 pldδ* mutants (Figure 2, E and F). To test this hypothesis, we determined membrane integrity by measuring electrolyte leakage and water loss in WT, *pldα1*, *pldδ*, and *pldα1 pldδ* rosettes at various time points during submergence or recovery. As shown in Figure 2G, the *pldα1*, *pldδ*, and *pldα1 pldδ* mutants exhibited significantly lower ionic leakage than WT when submerged for 4–8 days. In agreement with this result, the *pldα1*, *pldδ*, and *pldα1 pldδ* mutants also displayed significantly less water loss during postsubmergence reoxygenation compared to WT (Figure 2H).

To examine whether the phenotypes of submerged *pld* mutants were associated with ROS contents, we measured hydrogen peroxide (H₂O₂) levels in the rosettes of 4-week-old WT, *pldα1*, *pldδ*, and *pldα1 pldδ* plants upon submergence using an Amplex Red-based fluorescence assay. After submergence for 4 days and recovery for 6 h, the *pldα1*, *pldδ*, and *pldα1 pldδ* mutants had significantly lower H₂O₂ levels than WT exposed to the same conditions (Supplemental Figure S3A). We also determined malondialdehyde (MDA) levels as a measure of lipid peroxidation resulting from the accumulation of free radicals (Yuan et al.,

2017). Under normal conditions, MDA levels were comparable across all genotypes (Supplemental Figure S3B). After submergence, however, MDA levels were lower in the *pldα1*, *pldδ*, and *pldα1 pldδ* mutants relative to WT plants, in agreement with the lower H₂O₂ levels reported above (Supplemental Figure S3B).

PA binds to MPK3 and MPK6 and stimulates their kinase activity

To unravel the molecular mechanism behind the submergence-induced accumulation of PA, we set out to identify potential PA targets in the hypoxia signaling pathway. Previous studies have suggested that O₂ deprivation activates phosphorylation of MPK3 and MPK6 (Chang et al., 2012; Cho et al., 2016), with MPK6 being a possible target of PA (Yu et al., 2010). To establish a link between PA and the function of MPK3 and MPK6, we first examined the in vitro affinity of PA for recombinant MPK3 and MPK6 proteins by lipid overlay assays. As shown in Figure 3A, glutathione S-transferase (GST) alone did not bind the tested membrane lipids, but recombinant GST-MPK3 and GST-MPK6 proteins showed strong binding to PA and weak binding to PG in membrane lipid binding assays. In contrast, neither GST-MPK3 nor GST-MPK6 proteins showed any binding to PC, PE, PI, or PS in vitro (Figure 3A).

We independently validated the association of PA with MPK3 and MPK6 with in vitro pull-down assays using recombinant GST-MPK3 and GST-MPK6 proteins and PA beads (Figure 3B; Supplemental Figure S4A). As the control, PI beads failed to pull-down recombinant GST-MPK3 or GST-MPK6 (Supplemental Figure S4A). In addition, a recombinant GST fusion to the ABA receptor PYRABACTIN RESISTANCE1-LIKE4 (PYL4) showed no interaction with PA beads, as expected (Figure 3B). We then turned to microscale thermophoresis (MST) analysis, which showed that recombinant GST-MPK3 and GST-MPK6 bind PA with high affinities, as reflected by their dissociation constants (K_d) of 0.50 μ M and 0.11 μ M, respectively (Figure 3C; Supplemental S4B). However, neither recombinant protein was associated with PC, PI, or PS in MST analysis (Figure 3C; Supplemental S4B), suggesting that MPK3 and MPK6 specifically bind PA in vitro.

To confirm a role for MPK3 and MPK6 in the response to hypoxia, we tested the phosphorylation of MPK3 and MPK6 under light submergence or dark submergence conditions, two treatments that lead to hypoxia around the submerged plants (Chen et al., 2015). We established that under light submergence, MPK3 and MPK6 activity rapidly rose within 0.5 h, peaked after 1 h, and then returned to basal levels within 6 h after treatment (Figure 3, D and F). Consistent with this result, the phosphorylation of MPK3 and MPK6 was also activated 0.5 h into dark submergence, but not by dark treatment alone (Figure 3, E and F). In contrast, MPK3 and MPK6 protein levels did not change significantly under either submergence condition (Figure 3, D and E).

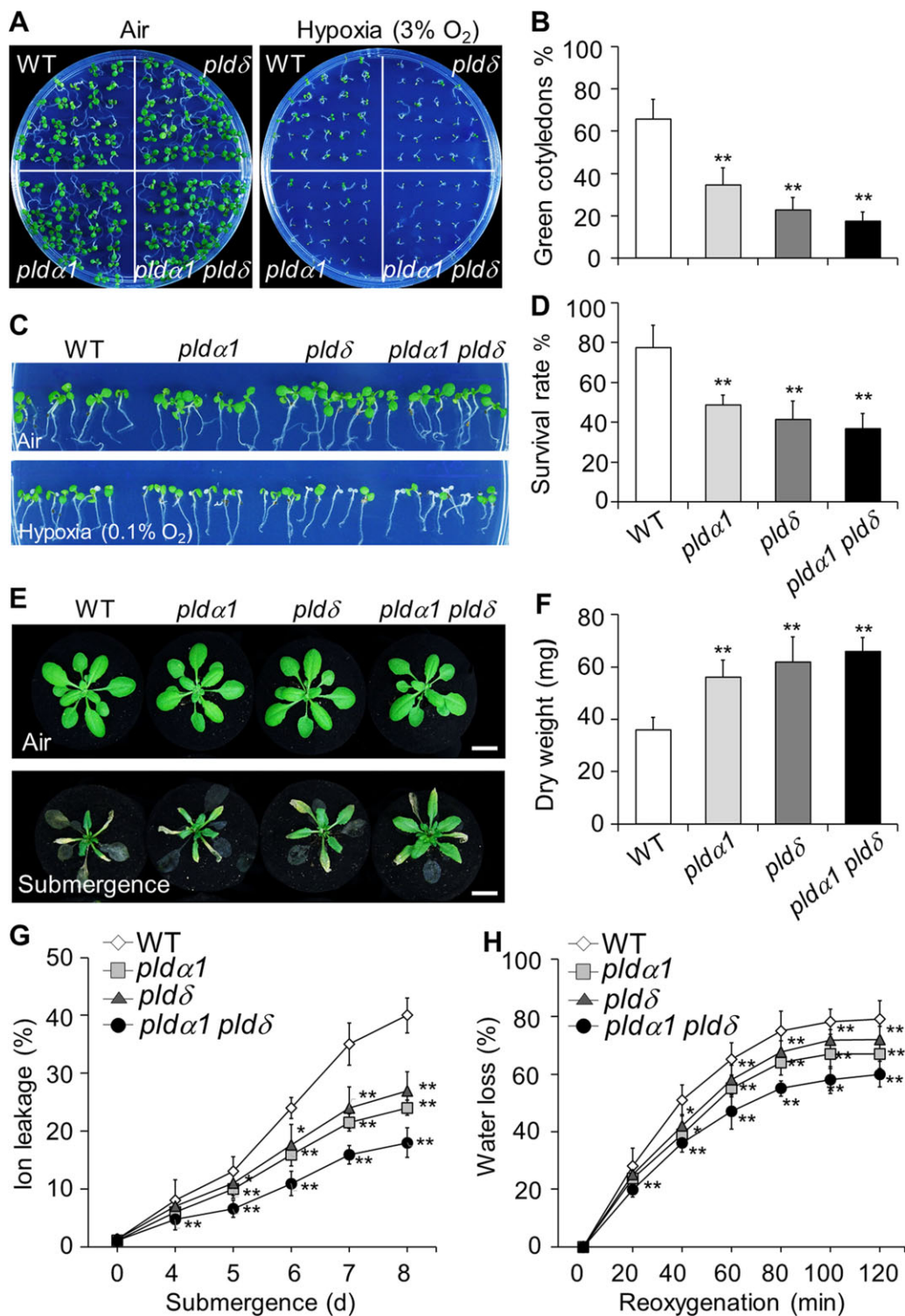


Figure 2 Knockouts in *PLDα1* and *PLDδ* result in increased sensitivity to hypoxia, but higher tolerance to submergence. A and B, Phenotypes (A) and percentage of seedlings with green cotyledons (B) for WT, *pldα1*, *pldδ*, and *pldα1 pldδ* seeds germinated under normoxia (air, 21% O₂) or hypoxia (3% O₂) conditions for 12 days. C and D, Phenotypes (C) and survival rates (D) of WT, *pldα1*, *pldδ*, and *pldα1 pldδ* seedlings grown under hypoxia (0.1% O₂) conditions. Six-day-old WT, *pldα1*, *pldδ*, and *pldα1 pldδ* seedlings grown on half-strength MS solid medium were transferred to normoxia (air) or hypoxia (0.1% O₂) for 5 days followed by recovery for 3 days under normal growth conditions. E and F, Phenotypes (E) and dry weights (F) of 4-week-old submerged WT, *pldα1*, *pldδ*, and *pldα1 pldδ* plants under submergence treatment. Plants were photographed before submergence (air) and after submergence treatment for 8 days, followed by 3 days recovery (submergence) under normal growth conditions. Dry weights were determined after recovery for 7 days. Bars, 1.5 cm. G and H, Ion leakage (G) and water loss (H) in 4-week-old WT, *pldα1*, *pldδ*, and *pldα1 pldδ* plants under light submergence treatment or after reoxygenation for the indicated times. All experiments were performed on three biological replicates. Data are means ± SD of three biological replicates. Asterisks indicate significant differences from WT (**P* < 0.05, ***P* < 0.01 by Student's *t* test).

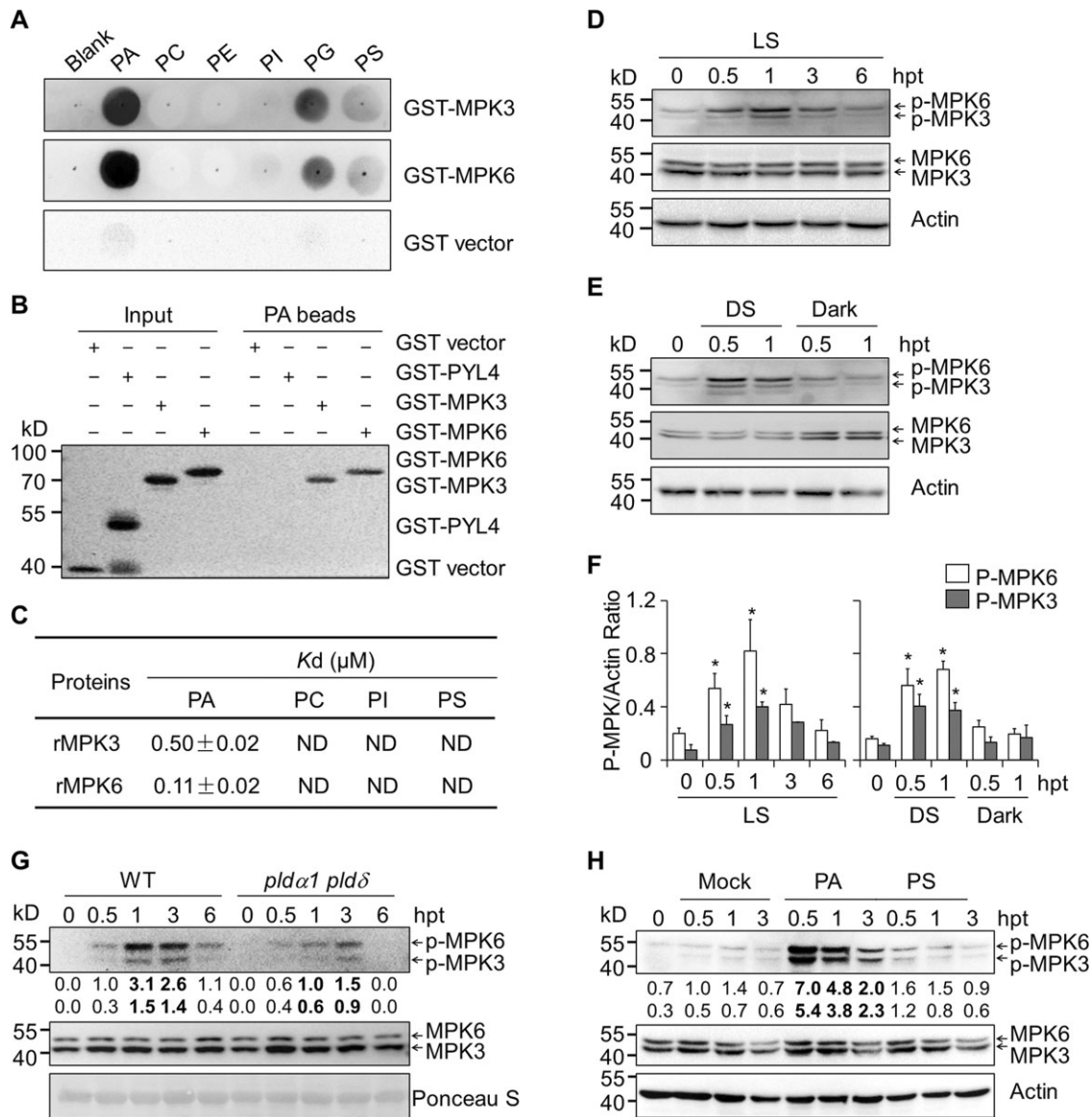


Figure 3 PA binds to MPK3 and MPK6 and enhances submergence-induced MPK3 and MPK6 activity. **A**, Lipid binding specificity of recombinant MPK3 and MPK6 proteins on membrane filters. About 50 μM of various lipids (PA, PC, PE, PI, PG, and PS dissolved in chloroform; natural lipid mixtures purified from soy, Avanti Polar Lipids) were spotted onto nitrocellulose membrane and incubated with 10 μg of purified GST-MPK3, GST-MPK6, or GST protein. Binding was detected by immunoblotting using an anti-GST antibody. Equal volume of chloroform was spotted as negative control (Blank). **B**, Pull-down assay showing the physical interaction between PA and recombinant MPK3 and MPK6 proteins. Recombinant proteins were incubated with PA beads, and the precipitated GST-MPK3 and GST-MPK6 were detected with anti-GST antibody. GST-PYL4 was used as a negative control. **C**, Dissociation constant (K_d) for the binding of recombinant MPK3 and MPK6 proteins to liposomes of PA, PC, PI, and PS (natural lipid mixtures purified from soy, Avanti Polar Lipids). A serial dilution of various liposomes ranging from 1.5 nM to 50 μM was prepared for mixing with the labeled proteins, and their binding affinities were measured by MST analysis. K_d , dissociation constant. ND, not detected. **D** and **E**, MPK3/MPK6 kinase activities were detected with anti-pTepY antibody. MPK3 and MPK6 proteins were detected with anti-MPK3 and anti-MPK6 antibodies, respectively. Actin, detected with an anti-actin antibody, was used as loading control. **F**, Quantification of MPK phosphorylation activity shown in (D) and (E). Data were calculated according to relative intensity from three independent experiments and the average values ± SD are shown. **G**, MPK3 and MPK6 kinase activities in WT and *pldα1 pldδ* plants and following submergence for 0.5, 1, 3, and 6 h. Total proteins were extracted and immunoblotting assays were performed using anti-pTepY, anti-MPK3, and anti-MPK6 antibodies, with Ponceau S-stained total protein as loading control. hpt, hour posttreatment. Relative intensity of each p-MPK3 or pMPK6 band normalized to the loading control is shown below. **H**, PA induces MPK3 and MPK6 activity in planta. Ten-day-old WT seedlings were treated without (Mock) or with 50 μM PA or PS liposomes (natural lipid mixtures purified from soy, Avanti Polar Lipids) for 0.5, 1, and 3 h, and immunoblotting assays were performed using anti-pTepY, anti-MPK3, anti-MPK6, and anti-actin antibodies, with actin as loading control. Relative intensity of each p-MPK3 or pMPK6 band normalized to the loading control is shown below. All experiments were performed on three biological replicates with similar results. Data in (C) and (F) are means ± SD of three biological replicates. Asterisks indicate significant differences from WT at 0 h (* $P < 0.05$ by Student's *t* test).

To confirm the influence of PA deficiency on submergence-activated phosphorylation of MPK3 and MPK6, we measured MPK3 and MPK6 levels in 4-week-old WT and *pldα1 pldδ* rosettes subjected to submergence for 0.5, 1, 3, or 6 h and compared them to protein levels in control plants that were not submerged. We observed significantly lower phosphorylation of both MPK3 and MPK6 in the *pldα1 pldδ* mutant compared to WT upon submergence at both time points (Figure 3G). Furthermore, we detected the phosphorylation of MPK3 and MPK6 in response to exogenous PA application. As shown in Figure 3H, compared to the mock control, application of PA liposomes, but not PS liposomes, activated MPK3 and MPK6 activities at 0.5, 1, and 3 h after treatment. These findings suggest that the submergence-induced accumulation of PA may be linked to the phosphorylation of MPK3 and MPK6 in Arabidopsis.

MPK3 and MPK6 positively regulate hypoxia responses

To further examine the physiological significance of MPK3 and MPK6 phosphorylation in hypoxia responses, we obtained two knockout mutants, *mpk3* (Yoo et al., 2008) and *mpk6* (Xu et al., 2008), for phenotypic analyses (Supplemental Figure S5, A and B). Given that a true *mpk3 mpk6* double loss-of-function mutation is embryo-lethal, we used the chemically inducible line *mpk3 mpk6-es* (estradiol-inducible silencing of MPK3 by RNA interference in the *mpk6* mutant background; Cheng et al., 2015). MPK3 and MPK6 mRNA levels and MPK3 and MPK6 protein levels in the *mpk3* or *mpk6* single mutants, as well as the *mpk3 mpk6-es* line, were significantly lower than in WT, as evidenced by PCR and immunoblot analyses (Supplemental Figure S5, C and D).

A careful phenotypic analysis revealed that under hypoxic (3% O₂) conditions, seed germination of the *mpk3* and *mpk6* single mutants and the *mpk3 mpk6-es* line on half-strength MS medium containing 10 μM β-estradiol is severely delayed relative to that of WT seeds (Figure 4A), which was also supported by the significantly reduced percentage of seedlings with green cotyledons seen in the mutant backgrounds (Figure 4B). In agreement with these results, the extent of hypoxia-induced leaf damage in the *mpk3* and *mpk6* single mutants and the *mpk3 mpk6-es* line was more severe than in WT seedlings (Figure 4C), as illustrated by the significantly reduced survival rates of the *mpk* plants upon reoxygenation (Figure 4D). Moreover, our submergence assays suggested that the *mpk3* and *mpk6* single mutants and the *mpk3 mpk6-es* line are more sensitive to submergence than WT (Figure 4E), as reflected by relative dry weights determined after recovery from submergence (Figure 4F). Compared to the *mpk3* and *mpk6* single mutants, the *mpk3 mpk6-es* line appeared to be more sensitive to both hypoxic and submergence stresses (Figure 4, A–F). Indeed, upon submergence for 4–8 days, ion leakage was measured for the rosettes of the *mpk3* and *mpk6* single mutants and the *mpk3 mpk6-es* line was significantly higher

than that of WT (Figure 4G). In addition, the *mpk3* and *mpk6* single mutants and the *mpk3 mpk6-es* line exhibited higher H₂O₂ levels than the WT after submergence for 3 days and recovery for 3 or 6 h (Figure 4H).

MPK3 and MPK6 phosphorylate RAP2.12 to enhance its transcription activity

Given that MPK3 and MPK6 may positively regulate hypoxia responses, we considered the potential interaction between MPK3 and MPK6 with members of ERF-VII family of transcription factors, which serve as key regulators of O₂ sensing in Arabidopsis (Gibbs et al., 2011; Licausi et al., 2011). Accordingly, we tested the potential association between MPK3 and MPK6 with RAP2.12 by in planta co-immunoprecipitation (Co-IP) assays. When HA-tagged RAP2.12 (RAP2.12-HA) was transiently co-transfected with FLAG-tagged MPK3 or MPK6 (MPK3-FLAG or MPK6-FLAG) in WT Arabidopsis protoplasts, we successfully immunoprecipitated the RAP2.12-HA fusion protein with anti-FLAG antibodies recognizing MPK3-FLAG and MPK6-FLAG proteins, but not with anti-FLAG magnetic beads alone (Figure 5A).

To determine whether MPK3 and MPK6 might regulate RAP2.12 stability, we then examined RAP2.12 protein levels in the same transient protoplast transfection assay. Compared to control samples transfected with RAP2.12-HA alone, we observed higher levels of the RAP2.12-HA fusion protein in protoplasts co-transfected with RAP2.12-HA and MPK3-FLAG or MPK6-FLAG (Figure 5B), suggesting that MPK3 and MPK6 stabilize RAP2.12 in vivo. In contrast, GFP-HA protein levels remained unchanged when GFP-HA was co-transfected with MPK3-FLAG or MPK6-FLAG, providing an important negative control (Figure 5B).

RAP2.12 is a core transcription factor involved in hypoxia signaling that activates the expression of hypoxia-responsive genes, including ALCOHOL DEHYDROGENASE1 (ADH1) (Fukao et al., 2006; Xu et al., 2006). To determine the effects of MPK3 and MPK6 on the transcriptional activity of RAP2.12, we performed a dual-luciferase (LUC) reporter assay in Arabidopsis protoplasts. We placed the firefly LUC reporter gene under the control of the ADH1 promoter to generate the ADH1_{pro}:LUC reporter (Supplemental Figure S6). We also constructed a series of effector constructs using the UBIQUITIN10 (UBQ10) promoter to drive the expression of RAP2.12 or MPK3 (Supplemental Figure S6). When appropriate combinations of these plasmids were co-transfected into Arabidopsis protoplasts, LUC activity measured from the ADH1_{pro}:LUC reporter was significantly higher relative to control samples (CK) when co-transfected with UBQ10_{pro}:RAP2.12, but much lower when ADH1_{pro}:LUC was co-transfected with UBQ10_{pro}:MPK3 (Figure 5C). Co-transfecting ADH1_{pro}:LUC with UBQ10_{pro}:RAP2.12 and UBQ10_{pro}:MPK3 resulted in intermediate LUC activity between that seen with transfection of either effector construct. However, exogenous application of PA to protoplasts co-transfected with both effectors increased LUC activity

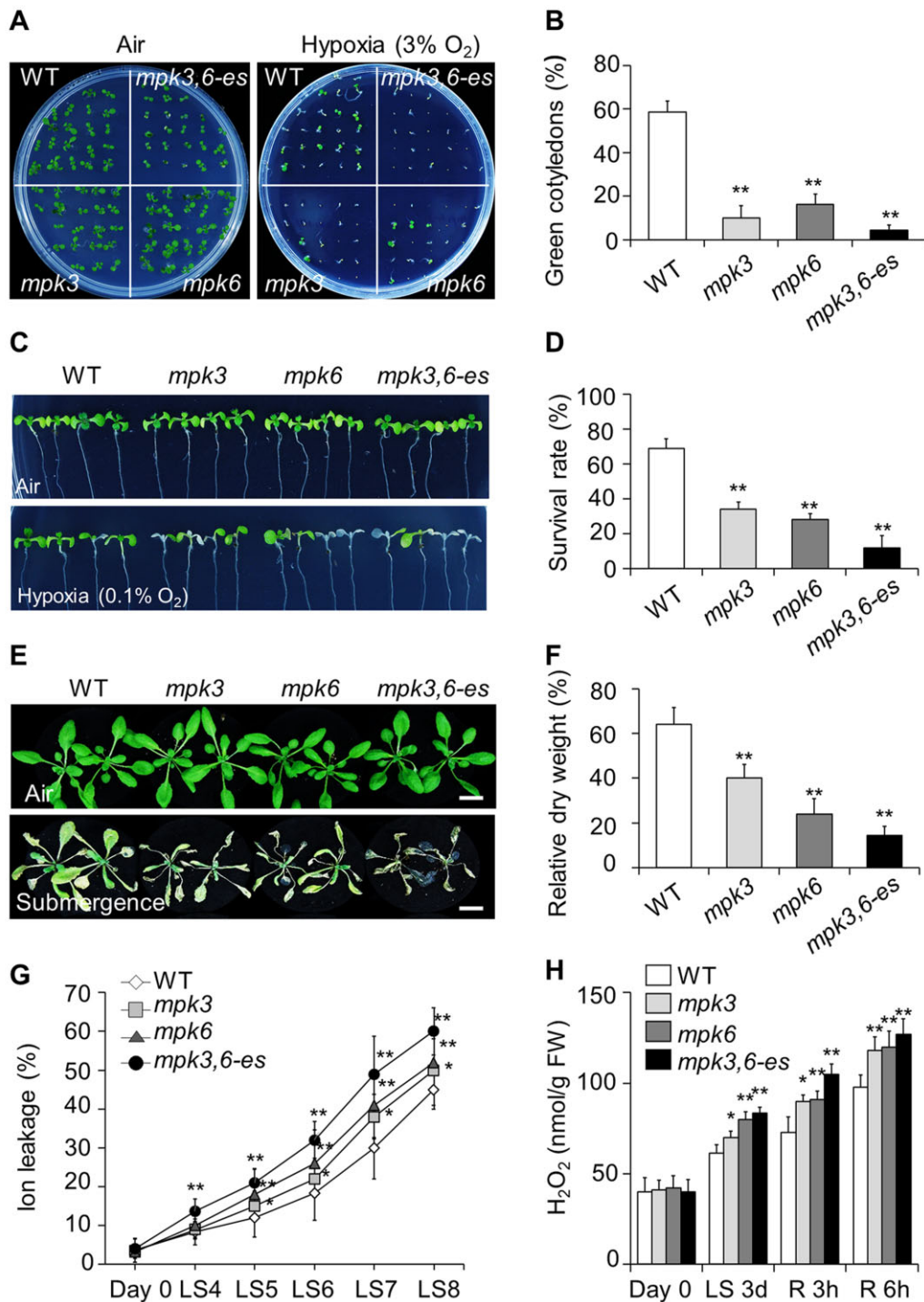


Figure 4 MPK3 and MPK6 are required for the regulation of plant tolerance to hypoxia and submergence. A and B, Phenotypes (A) and ratios of seedlings with green cotyledons (B) for WT, *mpk3*, *mpk6*, and *mpk3 mpk6-es* (*mpk3,6-es*) seedlings grown under 3% O₂ conditions. Seeds of WT, *mpk3*, *mpk6*, and *mpk3,6-es* were sown on half-strength MS medium with 10 μ M β -estradiol and germinated under normoxia (air) or hypoxia (3% O₂) for 10 days. C and D, Phenotypes (C) and survival rates (D) for WT, *mpk3*, *mpk6*, and *mpk3,6-es* seedlings grown under 0.1% O₂ exposure. Six-day-old WT, *mpk3*, *mpk6*, and *mpk3,6-es* seedlings grown on MS solid medium were transferred to MS medium containing 10 μ M estradiol, and continued to grow under normoxia (air) or hypoxia (0.1% O₂) for 5 days followed by recovery for 3 days. E and F, Phenotypes (E) and dry weights (F) of 4-week-old submergence-treated WT, *mpk3*, *mpk6*, and *mpk3,6-es* plants. Plants were photographed before submergence (air) and after submergence for 8 days, followed by 3 days recovery (submergence). Dry weights were calculated after recovery for 7 days. Bars: 1.5 cm. G and H, Ion leakage (G) and H₂O₂ levels (H) in 4-week-old WT, *mpk3*, *mpk6*, and *mpk3,6-es* plants before submergence (Day 0) and after LS treatment followed by recovery (R) for the indicated times. All experiments were performed on three biological replicates with similar results, and average data calculated from three biological replicates are shown. Data are means \pm SD of three independent biological replicates. Asterisks indicate significant differences from WT (**P* < 0.05, ***P* < 0.01 by Student's *t* test).

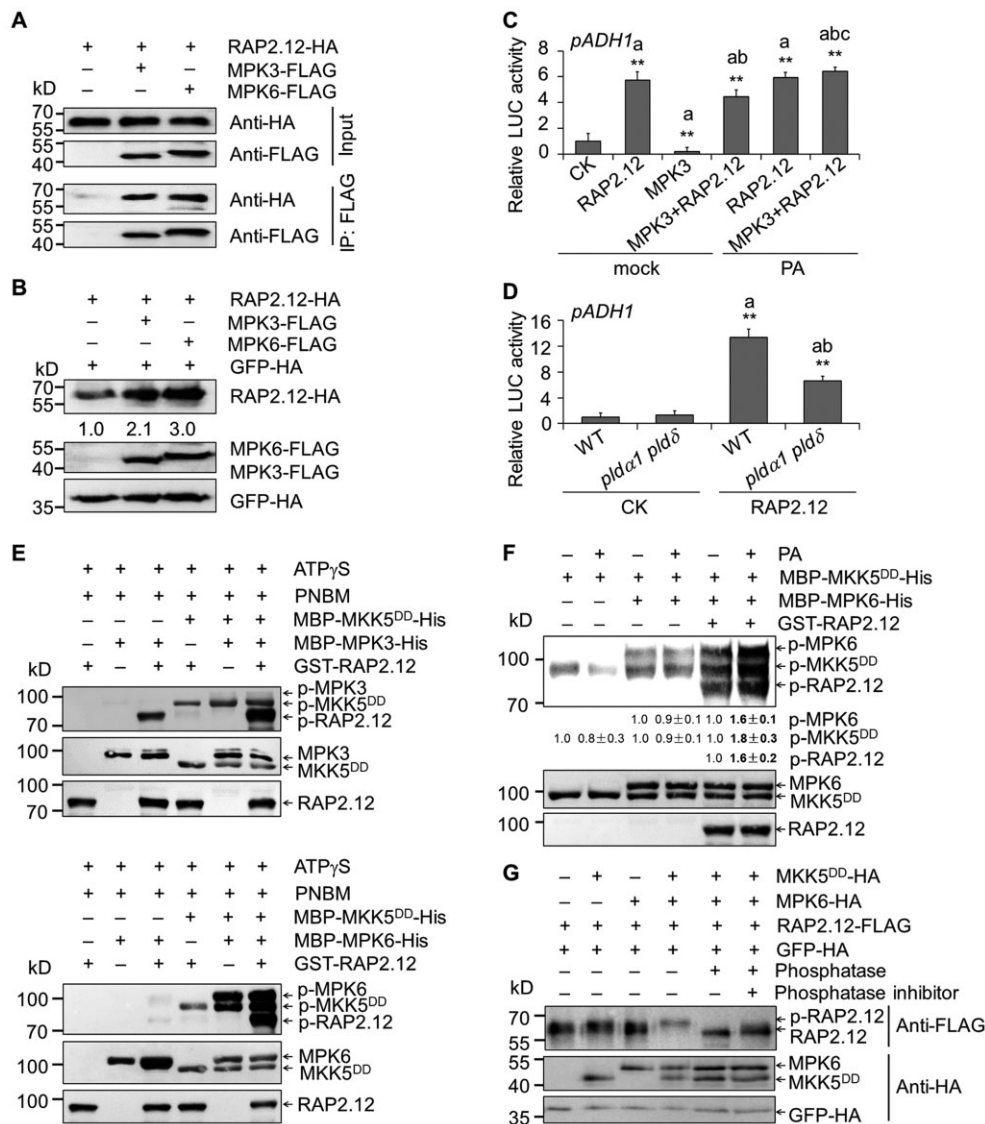


Figure 5 PA enhances MPK3- and MPK6-mediated phosphorylation of RAP2.12 to activate its transcriptional activity. **A**, Co-IP assay showing the interaction between MPK3/MPK6 and RAP2.12. Constructs encoding *MPK3-FLAG* and *MPK6-FLAG*, and *RAP2.12-HA* were transiently transfected in WT Arabidopsis protoplasts and immunoprecipitated with anti-FLAG beads. **B**, Immunoblot analyses showing RAP2.12 protein levels when co-expressed with MPK3 or MPK6. *RAP2.12-HA* was co-transfected with or without *MPK3-FLAG* or *MPK6-FLAG* in WT Arabidopsis protoplasts overnight. pUC119-eGFP-HA was co-transfected to determine transfection efficiency for each sample. Anti-HA and anti-FLAG antibodies were used for immunoblotting. Relative intensity of each protein band normalized to the GFP-HA control is shown below. **C**, Dual-LUC reporter assay showing RAP2.12-activated transcription of *ADH1* in the absence (mock) or presence of PA. When indicated, protoplasts were treated with 10- μ M PA liposomes (natural lipid mixture purified from soy, Avanti Polar Lipids) for 16 h. “a” indicates significantly higher or lower levels than in control; “b” indicates significantly higher or lower levels than with RAP2.12 alone; “c” indicates significantly higher or lower levels than in mock-treated protoplasts. **D**, Dual-LUC reporter assays showing RAP2.12-activated transcription of *ADH1* in WT and *pldα1 pldδ* protoplasts. “a” indicates significantly higher or lower levels than controls not co-transfected with RAP2.12 (CK), “b” indicates significantly higher or lower levels than RAP2.12 in WT. **E**, Activated MPK3 and MPK6 phosphorylate RAP2.12 in vitro. Phosphorylated recombinant MPK3, MPK6, MKK5^{DD}, as well as RAP2.12 were detected with anti-thiophosphate ester rabbit monoclonal antibodies after gel electrophoresis (top), recombinant MKK5^{DD}, MPK3, and MPK6 were detected with anti-His antibody (middle), and recombinant RAP2.12 was detected with anti-GST antibody (bottom). Reactions lacking the specified components (–) were used as controls. Recombinant proteins were separated by 10% SDS–PAGE after incubation in protein kinase buffer containing ATP_γS and PNBM. **F**, MPK6-mediated RAP2.12 phosphorylation is enhanced by the application of PA. Phosphorylated recombinant MPK6 and MKK5^{DD}, as well as RAP2.12 were detected with anti-thiophosphate ester rabbit monoclonal antibodies after gel electrophoresis (top), recombinant MKK5^{DD} and MPK6 were detected with anti-His antibody (middle), and recombinant RAP2.12 was detected with anti-GST antibody (bottom). Reactions lacking the specified components (–) were used as controls. Recombinant proteins were separated by 10% SDS–PAGE after incubation in protein kinase buffer containing ATP_γS and PNBM. Relative intensity of phosphorylated proteins normalized to the control is shown below. **G**, Phosphorylation of RAP2.12 by MPK6 in vivo. Constructs encoding MKK5^{DD}-HA and MPK6-HA, and RAP2.12-FLAG were transiently transfected in Arabidopsis protoplasts. Proteins were extracted 16 h after incubation to allow protein accumulation. The phosphorylation of RAP2.12 was confirmed by incubation with phosphatase and phosphatase inhibitor, and the immunoblots were probed with anti-HA and anti-FLAG antibodies. All experiments were performed on three biological replicates with similar results. For all blots, numbers on the left indicate the molecular weight (kDa) of each band. For the LUC reporter assay, data are means \pm SD of three independent experiments. Asterisks indicate significant differences from WT (***P* < 0.01 by Student’s *t* test).

compared to the mock control (Figure 5C). To obtain an independent validation of PA regulating RAP2.12-mediated induction of *ADH1* transcription, we repeated the co-transfection assays in *pldα1 pldδ* mutant protoplasts. As shown in Figure 5D, LUC activity derived from the *ADH1_{pro}:LUC* reporter was about half that of the activity measured in WT protoplasts. These results indicate that transcriptional control of *ADH1* by RAP2.12 is dependent on PA-activated MPK3 and/or MPK6.

Because MPK3 and MPK6 activity was rapidly activated upon submergence (Figure 3), we next tested whether RAP2.12 might be a substrate for phosphorylation by MPK3 and MPK6. As shown in Supplemental Figure S7A, both MPK3 and MPK6 phosphorylated RAP2.12 in the presence of ATP γ S and *p*-nitrobenzyl mesylate (PNBM) in vitro. MKK5 is an upstream MAPKK associated with MPK3 and MPK6 to form the well-studied MKK5–MPK3/MPK6 cascade, which is implicated in plant response to diverse environmental stresses (Meng and Zhang, 2013). To investigate the possible requirement for a MAPKK in the MPK3/MPK6-mediated phosphorylation of RAP2.12, we included the constitutively active MKK5^{DD} (Zhao et al., 2017) in the in vitro phosphorylation assay. As shown in Figure 5E, recombinant MBP–MPK3 and MBP–MPK6 phosphorylated RAP2.12 more in the presence of MKK5^{DD} than in the samples lacking MKK5^{DD}. The pMPK3 signal is much less than the pMKK5^{DD} signal (Figure 5E; upper), likely due to the overlap between the pMPK3 and MKK5^{DD} bands. As positive and negative controls (Meng et al., 2013; Zhou et al., 2020), MBP–MPK6 protein phosphorylated ERF6, but did not phosphorylate ACBP1 in vitro, as expected (Supplemental Figure S7, B and C).

We next analyzed the amino acid sequence of RAP2.12 and found six potential MAPK phosphorylation sites (Thr-86, Ser-87, Thr-88, Ser-210, Thr-280, and Thr-313) (Supplemental Figure S8A). When all six Thr/Ser residues were mutated to Ala (RAP2.12^{6A}), RAP2.12 failed to be phosphorylated by the MKK5–MPK3/MPK6 cascade (Supplemental Figure S8B).

To further test the role of PA in the MKK5–MPK3/MPK6-mediated phosphorylation of RAP2.12, we included PA in the in vitro phosphorylation assay. Our data showed that PA enhanced the activity of MPK6 to phosphorylate RAP2.12 (Figure 5F). Intriguingly, we observed that PA also activated MKK5 in vitro (Figure 5F), suggesting that PA may affect multiple steps in this phosphorylation cascade. To test the specific effect of PA on the phosphorylation of RAP2.12, we performed an in vitro phosphorylation assay by first phosphorylating MPK6 by MKK5^{DD} in the presence of only unlabeled (“cold”) ATP for 1 h to ensure activation of MPK6 by MKK5^{DD}. Then, we added PA, ATP γ S, and PNBM to finish the protein kinase reaction and separated the proteins by 10% sodium dodecyl sulfate polyacrylamide gel electrophoresis (SDS–PAGE). Compared to the reaction without PA, the presence of PA stimulated MPK6-mediated phosphorylation of RAP2.12 in vitro (Supplemental Figure S8C).

To examine whether MPK3 and MPK6 phosphorylate RAP2.12 in vivo, we co-transfected the HA-tagged MKK5^{DD} and MPK6 (MKK5^{DD}-HA, MPK6-HA), and FLAG-tagged RAP2.12 (RAP2.12-FLAG) constructs into Arabidopsis protoplasts. Immunoblot analyses suggested that the activation of MPK6-HA by MKK5^{DD}-HA resulted in RAP2.12 shifting to a higher molecular weight band, and this shift was completely abolished by the addition of a phosphatase (Figure 5G), suggesting that MPK3 and MPK6 phosphorylate RAP2.12 in vivo.

MPK3 and MPK6 feedback regulate PLD α 1 and PLD δ stability and submergence-induced PA production

To determine whether MPK3 and MPK6 may be involved in feedback regulation of PLD α 1 and PLD δ in response to hypoxia, we tested their protein–protein interactions using CoIP and bimolecular fluorescence complementation (BiFC) assays. As shown in Figure 6A, HA-tagged MPK3 and MPK6 (MPK3-HA and MPK6-HA) were co-immunoprecipitated by FLAG-tagged PLD α 1 and PLD δ (FLAG-PLD α 1 and FLAG-PLD δ) in vivo. Moreover, we detected an interaction between the kinases (MPK3 and MPK6) and the phospholipases (PLD α 1 and PLD δ) by BiFC in Arabidopsis protoplasts (Figure 6B). When MPK3-*nYELLOW FLUORESCENT PROTEIN* (YFP) or MPK6-*nYFP* and PLD α 1-*cYFP* or PLD δ -*cYFP* were transiently co-transfected in WT protoplasts, we observed YFP fluorescence, which is evidence of BiFC, in the cytoplasm and at the plasma membrane (Figure 6B). In contrast, co-transfection of the negative controls MPK3-*nYFP/cYFP*, MPK6-*nYFP/cYFP*, and PLD α 1-*nYFP/CPK12-cYFP*, MPK9-*nYFP/PLD δ -cYFP* failed to reconstitute intact YFP in Arabidopsis leaf protoplasts and yielded no detectable fluorescence (Supplemental Figure S9).

Since MPK3/MPK6 and PLD α 1/PLD δ interact, we hypothesized that PLD α 1 and PLD δ might themselves be substrates for MPK3- and MPK6-mediated phosphorylation. To test this hypothesis, we purified recombinant GST-MPK3, GST-MPK6, GST-PLD α 1, and GST-PLD δ proteins, and performed in vitro phosphorylation assays. As shown in Figure 6C, GST-MPK3 and GST-MPK6 phosphorylated GST-PLD α 1 and GST-PLD δ in the presence of ATP γ S and PNBM. To identify the phosphorylation sites of PLD α 1, we enriched the FLAG-PLD α 1 proteins from 2-week-old *UBQ10_{pro}:FLAG-PLD α 1* transgenic plants by IP followed by mass spectrometry. We identified the two residues Ser-481 and Ser-776 as potential in vivo MAPK phosphorylation sites in PLD α 1 (Supplemental Figure S10).

Using immunoblot analysis with anti-PLD α 1-specific antibodies, we then determined that before submergence and after submergence for 1, 3, or 6 h, PLD α 1 proteins accumulate in seedlings from the *mpk3 mpk6-es* line to higher levels than in WT seedlings (Figure 6D). Furthermore, there were few differences in the levels of phospholipids including PC, PE, and PA, between WT and *mpk3 mpk6-es* mutant plants under normoxic conditions, as determined by lipid profiling

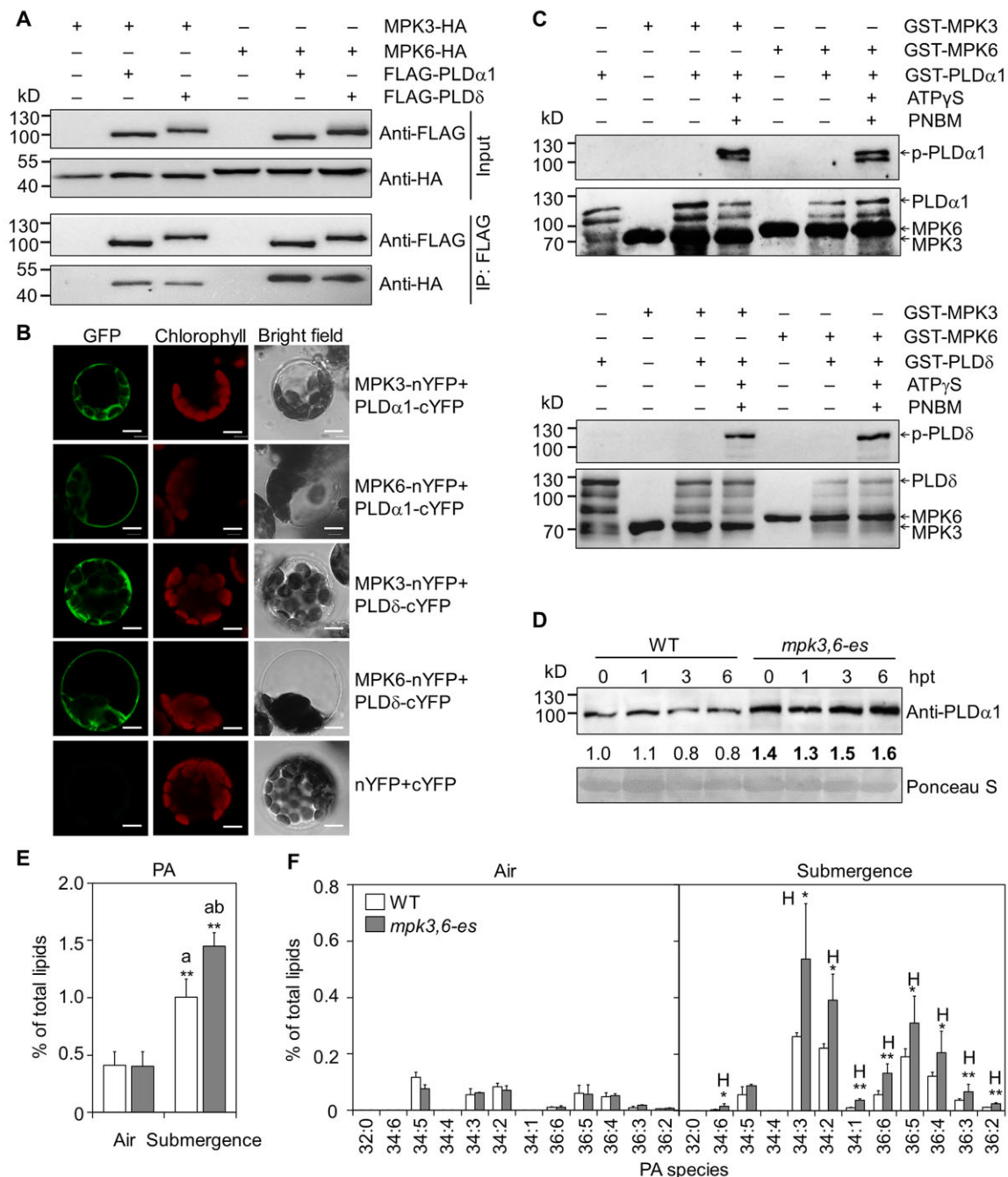


Figure 6 MPK3 and MPK6 feedback-regulate PLD α 1 and PLD δ to modulate submergence-induced PA accumulation. A, Co-IP assay showing the interaction between MPKs (MPK3 and MPK6) and PLDs (PLD α 1 and PLD δ) in vivo. Constructs encoding MPK3-HA and MPK6-HA and FLAG-PLD α 1 and FLAG-PLD δ were transiently co-transfected in WT Arabidopsis protoplasts and immunoprecipitated with anti-FLAG beads. B, BiFC assay of MPKs (MPK3 and MPK6) and PLDs (PLD α 1 and PLD δ) in Arabidopsis. Constructs encoding split YFP, nYFP and cYFP fusions MPKs-nYFP (MPK3-nYFP and MPK6-nYFP) and PLDs-cYFP (PLD α 1-cYFP and PLD δ -cYFP) were co-transfected in WT Arabidopsis protoplasts for 16 h under normal light–dark conditions. Confocal images for yellow fluorescent protein (YFP), chlorophyll autofluorescence, and bright field are shown. Bars, 10 μ m. C, MPK3 and MPK6 phosphorylate PLD α 1 and PLD δ in vitro. Phosphorylated PLD was detected with anti-thiophosphate ester rabbit monoclonal antibody after gel electrophoresis (top), recombinant MPK3, MPK6, and PLD α 1 and PLD δ were detected with anti-GST antibody (bottom). Reactions lacking the specified components (–) were used as controls. Recombinant proteins were separated by 10% SDS–PAGE after incubation in protein kinase buffer containing ATP γ S and PNBM. D, MPK3 and MPK6 negatively regulate PLD α 1 protein levels in response to submergence. Ten-day-old WT and *mpk3,6-es* seedlings were subjected to submergence for the indicated times. The immunoblots were probed with PLD α 1-specific antibodies, with Ponceau S-stained total protein as loading control. E and F, The loss of MPK3 and MPK6 results in PA accumulation in response to submergence. Levels of total PA (E) and various PA species (F) were measured from the rosettes of 4-week-old WT and *mpk3,6-es* plants before submergence (air) and after 48-h submergence treatment (submergence). a, indicates significant differences when compared to that of 0 h; b indicates significant differences when compared to that of WT, respectively. Lipid profiling analyses were performed on three biological replicates with similar results. Values represent means \pm SD ($n = 4$) of four independent biological replicates, and each replicate was collected from the rosettes of at least seven plants. Asterisks with “H” indicate significantly higher than WT for each PA species (* $P < 0.05$, ** $P < 0.01$ by Student’s t test).

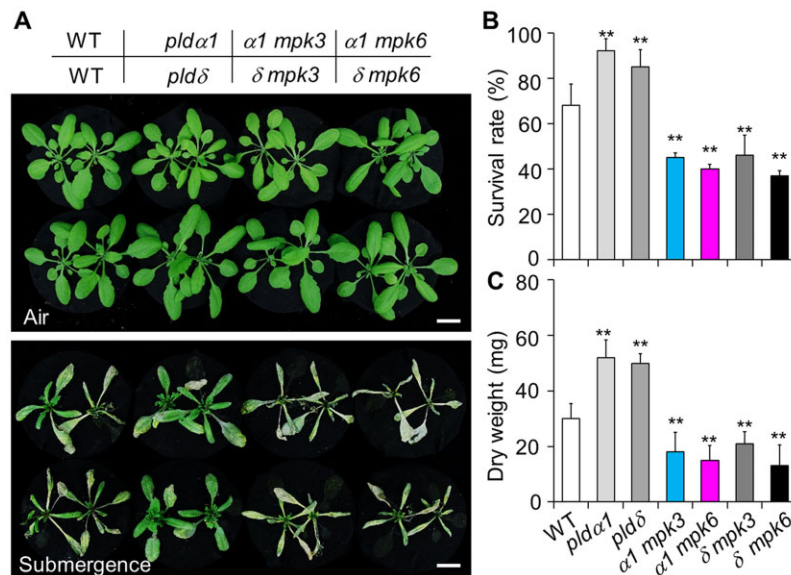


Figure 7 Loss of MPK3 or MPK6 suppresses the submergence-tolerant phenotypes of *pldα1* and *pldδ* mutants. Phenotypes (A), survival rates (B), and dry weights (C) of WT, *pldα1*, *pldδ*, *pldα1 mpk3* (*α1 mpk3*), *pldα1 mpk6* (*α1 mpk6*), *pldδ mpk3* (*δ mpk3*), and *pldδ mpk6* (*δ mpk6*) plants upon submergence treatment. Four-week-old plants were photographed before submergence (air) and after 8 days submergence, followed by 3 days recovery (submergence). Survival rates and dry weights were calculated after recovery for 7 days. Bars, 1.5 cm. All experiments were performed on three biological replicates with similar results. Data in (B) and (C) are means \pm SD of three biological replicates. Asterisks indicate significant differences from WT (* $P < 0.05$, ** $P < 0.01$ by Student's *t* test).

(Figure 6E; Supplemental Figure S11). However, we found that total PA levels were significantly higher in the *mpk3 mpk6-es* line than in WT after submergence for 48 h (Figure 6E). In particular, the levels of 34:6-, 34:3-, 34:2-, 34:1-, 36:6-, 36:5-, 36:4-, 36:3-, and 36:2-PA species were higher in the *mpk3 mpk6-es* line relative to WT (Figure 6F). In contrast, the total levels of PC and some species of PC and PE were significantly lower in the *mpk3 mpk6-es* line compared to WT under submergence (Supplemental Figure S11).

To determine the genetic relationship between PLDs (PLD α 1 and PLD δ) and MPKs (MPK3 and MPK6) in plant responses to hypoxia, we generated the double mutants *pldα1 mpk3*, *pldα1 mpk6*, *pldδ mpk3*, and *pldδ mpk6* by crossing the *pldα1* or *pldδ* single mutants with the *mpk3* or *mpk6* single mutants. Four-week-old *pldα1* and *pldδ* single mutants showed higher tolerance to light submergence for 8 days when compared to WT (Figure 7A). In contrast, the *pldα1 mpk3*, *pldα1 mpk6*, *pldδ mpk3*, and *pldδ mpk6* double mutants were hypersensitive to submergence (Figure 7A), thus recapitulating the phenotypes seen in the *mpk3* and *mpk6* single mutants (Figure 4). This result was further supported by the survival rates and dry weights of all genotypes after submergence (Figure 7, B and C). These findings suggest that PLD α 1- and PLD δ -mediated PA signaling acts upstream of MPK3 and MPK6 during plant responses to submergence. Taken together, our findings suggest that MPK3 and MPK6 interact with and phosphorylate PLD α 1 and PLD δ , which may contribute to feedback inhibition of PA production under submergence.

Discussion

Increasing evidence suggests that PA is a key lipid messenger in plant responses to multiple biotic and abiotic stresses, including pathogen infections, cold, wounding, high salt, and heat stress (Katagiri et al., 2001; Li et al., 2004; Zhang et al., 2009, 2013, 2017; Bargmann et al., 2009a, 2009b; Yu et al., 2010; Pinosa et al., 2013; Hyodo et al., 2015; Yao and Xue, 2018). We and other groups have recently demonstrated in various species that PA accumulates in submerged plants (Xie et al., 2015a; Wang et al., 2016; Xu et al., 2020), supporting the notion that PA may share a conserved function in hypoxia responses across the plant kingdom. However, the molecular mechanism behind the regulation of submergence-induced hypoxia signaling by PA remains unknown.

In this study, we present several lines of evidence to show that PA regulates plant tolerance to submergence by modulating both membrane integrity and MPK3/6-mediated hypoxia signaling. First, the accumulation of PA in response to PLD α 1- and PLD δ -mediated hydrolysis of PE was induced by submergence, and returned to basal levels during postsubmergence reoxygenation (Figure 1). Second, phenotypic analyses showed that the *pldα1* and *pldδ* single mutants and the *pldα1 pldδ* double mutant exhibit attenuated tolerance to a low O₂ environment, but enhanced resistance to submergence, the latter likely due to improved membrane integrity in these PA-deficient mutants (Figure 2). Third, we determined that PA can bind to recombinant MPK3 and MPK6 proteins in vitro and can modulate their activity

in vivo (Figure 3). Fourth, MPK3 and MPK6 phosphorylated the key transcription factor RAP2.12 and activated its PA-dependent transcriptional activity (Figure 5). Finally, MPK3 and MPK6 interacted with PLD α 1 and PLD δ and formed a regulatory feedback loop that modulated their stability (Figure 6). Consistent with this last result, we discovered that the *mpk3* and *mpk6* single mutants are hypersensitive to hypoxia and completely suppress the submergence-tolerant phenotypes of *pld α 1* and *pld δ* mutants (Figures 4 and 7). Thus, our findings reveal a PA–MPK3/6–RAP2.12 regulatory module that is required for plant hypoxia responses.

PA is a polar lipid lacking a head group and may affect cell membrane properties due to its unique chemical structure. For instance, when plants experience cold/freezing temperatures, they accumulate PA, as well as lipid molecules with a small head group such as monogalactosyl-diacylglycerol or DAG. These lipids tend to form a destabilized H_{II}-type lipid phase, which results in the shrinkage of membrane structures and ionic leakage, and further attenuates plant tolerance to the imposed stress (Kuiper, 1970; Verkleij et al., 1982; Thomashow, 1999; Welti et al., 2002; Moellering et al., 2010; Moellering and Benning, 2011; Tan et al., 2018). Consistent with this notion, the *pld α 1* mutants show enhanced tolerance to freezing temperatures and the *PLD α 1*-overexpressing lines are more sensitive to freezing temperatures (Welti et al., 2002; Rajashekar et al., 2006). Conversely, removal of these lipids in mutants such as *dgk2*, *dgk3*, and *dgk5*, confers improved freezing tolerance and decreased PA production (Tan et al., 2018).

Our current findings suggest that the PA-deficient mutants *pld α 1*, *pld δ* , and their double mutant *pld α 1 pld δ* exhibit increased sensitivity to hypoxia, but enhanced tolerance to submergence, along with significantly lower water loss, ionic leakage, and ROS accumulation when submerged (Figure 2; Supplemental Figure S3). It is therefore conceivable that, similar to its role in plant response to cold/freezing stress, PA is involved in regulating submergence tolerance by determining cell membrane structures or ROS-induced cell death. Previous studies have suggested that through the downregulation of genes involved in cuticular lipid biosynthesis, the land plant *Arabidopsis* increases the permeability of its cuticle under submergence conditions, thus helping plants cope with the lack of O₂ (Kim et al., 2017). More recent findings indicate that in addition to its role in modulating Group VII ethylene response factor (ERF-VII) signaling, the long-chain acyl-CoA synthetase LACS2 confers tolerance to submergence by affecting cuticle surface structures in *Arabidopsis* (Xie et al., 2020; Zhou et al., 2020). Taken together, these observations provide strong evidence to support the idea that lipid molecules (including PA) are critical for regulating plant acclimation to hypoxia, including morphological and anatomical changes that improve the survival of submerged plants. Given that PA can also be synthesized by DGK by phosphorylating DAG outside of the PLD pathway (Gómez-Merino et al., 2004; Arisz et al., 2009; Tan et al.,

2018), determining whether DGKs and the pool of PA derived from DGKs are involved in plant hypoxia responses will deepen our understanding of the role of PA in plant hypoxia acclimation. Interestingly, transcript levels of *DGK1* and *DGK5* were rapidly upregulated within 10 min after submergence, in contrast to the lagging induction of *PLD α 1* and *PLD δ* upon submergence after 3 and 48 h (Supplemental Figure S1), suggesting that the short-term accumulation of PA is likely derived from PA catalyzed by DGKs, although their biological significance remains to be further investigated.

PC and PE are known substrates for PLD hydrolysis and PA production in *Arabidopsis* (Wang et al., 2006); however, our data suggested that upon submergence, only PE levels were significantly higher in the *pld* mutants relative to WT (Table 1 and Figure 1B), but PC and PE levels were reduced in submerged WT after 48 h (Figure 1A; Xie et al., 2015a, 2015b). These findings indicate that PE, but not PC, is likely a PLD α 1/PLD δ substrate in the response to plant submergence. Consistent with this, a previous kinetic study showed that *Arabidopsis* PLD δ prefers PE rather than PC with V_{\max}/K_m values 50 and 7.7, respectively (Qin et al., 2002). Alternatively, de novo biosynthesis of PC and PE may mask the hydrolysis of these two phospholipids, which may thus compensate for their decrease, particularly at the short-term submergence stages within minutes to hours. Moreover, given that PLDs can transphosphatidylate ethanol to produce phosphatidylethanol (Wang et al., 2006), the accumulation of ethanol through anaerobic respiration may also contribute to PE production under long-term submergence conditions.

Previous studies have revealed that PA primarily acts as a signaling molecule by targeting substrate proteins such as ABA INSENSITIVE 1, RbohD/F, MONOGALACTOSYL DIACYLGLYCEROL SYNTHASE 1, SPHINGOSINE KINASE1/2, CONSTITUTIVE TRIPLE RESPONSE1 (CTR1), and MPK6 to regulate their various activities (Zhang et al., 2004, 2009; Testerink et al., 2007; Dubots et al., 2010; Yu et al., 2010; Guo et al., 2011; McLoughlin and Testerink, 2013). In particular, PA binds to the kinase domain of CTR1 in vitro and inhibits its kinase activity in vivo (Testerink et al., 2007; Xie et al., 2015a), indicating that PA may participate in hypoxia responses by modulating CTR1 activity along the ethylene signaling pathway (Xie et al., 2015a). Moreover, the PA–CTR1 interaction promotes the processing and nuclear translocation of ETHYLENE INSENSITIVE2 (EIN2), whose activity is directly regulated by CTR1 in ethylene signaling (Xie et al., 2015a). Moreover, PA interacts with and stimulates MPK6, which in turn mediates the phosphorylation of the downstream target Na⁺/H⁺ antiporter SOS1, thereby conferring salinity tolerance to *Arabidopsis* (Yu et al., 2010). Here, we further observed that PA might function in hypoxia signaling by interacting with MPK3 and MPK6 to activate their kinase activity as well as their downstream signal transduction cascades (Figure 3). Given that CTR1 blocks MPK3 and MPK6 activation and simultaneously promotes

EIN3 degradation by distinct MPK phosphorylation (Yoo et al., 2008), it is therefore possible that PA may function either as an adaptor or an integrator in maintaining the dynamics of the CTR1–MPK3/6 complex during plant responses to hypoxia. Moreover, we observed that MKK5 is likely an important upstream regulator that enhances phosphorylation of RAP2.12 by MPK3 and MPK6 (Figure 5E). In addition to MPK3 and MPK6, PA also activated MKK5 in vitro (Figure 5F), suggesting that PA may have multiple regulatory roles in the hypoxia signaling cascade in plants.

The importance of MPK3 and MPK6 in hypoxia signaling has been previously reported in Arabidopsis and rice (Chang et al., 2012; Singh and Sinha, 2016). In rice, MPK3 specifically interacts with the ERF-like protein SUB1A to form a positive feedback loop, thus contributing to submergence tolerance (Singh and Sinha, 2016). In Arabidopsis, the activity of MPK3, MPK4, and MPK6 is rapidly induced upon O₂ deprivation as well as during reoxygenation (Chang et al., 2012). Overexpression of Arabidopsis MPKs (MPK3, MPK4, and MPK6) confers tolerance to hypoxic stress. However, the transient activation of MPK6 triggered by O₂ deprivation does not lead to a significant induction of the core mRNAs associated with hypoxia responses (Chang et al., 2012). Our results presented herein further extend the significance of MPK3 and MPK6 to the regulation of hypoxia tolerance in plants. We observed that MPK3 and MPK6 directly interacted with the ERF-VII transcription factor RAP2.12 to activate its transcriptional activity (Figure 5), suggesting that MPK3 and MPK6 redundantly function as conserved upstream regulators in modulating the stability and activity of ERF-VII transcription factors in both monocot and dicot plant species.

Previous findings have revealed that besides PLD α 1-derived PA, PLD α 1 itself physically associates with MPKs (Yu et al., 2010; Vadovič et al., 2019), although the physiological significance of this interaction remains unclear. We observed that the hypoxia-triggered activity of MPK3 and MPK6 was suppressed in the *pld α 1 pld δ* double mutant (Figure 3), suggesting that PA derived from PLD activity is required for hypoxia-induced MPK3/6 activation. Moreover, upon submergence, we noticed that PLD α 1 protein levels were significantly higher in the *mpk3 mpk6-es* inducible line relative to WT plants (Figure 6D). Biochemical analyses showed that MPK3 and MPK6 directly interact with and phosphorylate PLD α 1 and PLD δ (Figure 6, A–C), suggesting that MPK3/6 form a regulatory feedback loop with PLD α 1 and/or PLD δ to suppress their activity, which may play an important role in maintaining PA production at a proper level, especially when the plant is experiencing long-term submergence. Consistent with this, the *mpk3,6-es* double mutant accumulated PA levels during submergence due to the feedback suppression of PLDs by MPK3 and MPK6 (Figure 6). This accumulated PA may further disturb membrane integrity and result in the *mpk3,6-es* double mutants being hypersensitive to both hypoxia and submergence (Figure 4). Notably, in

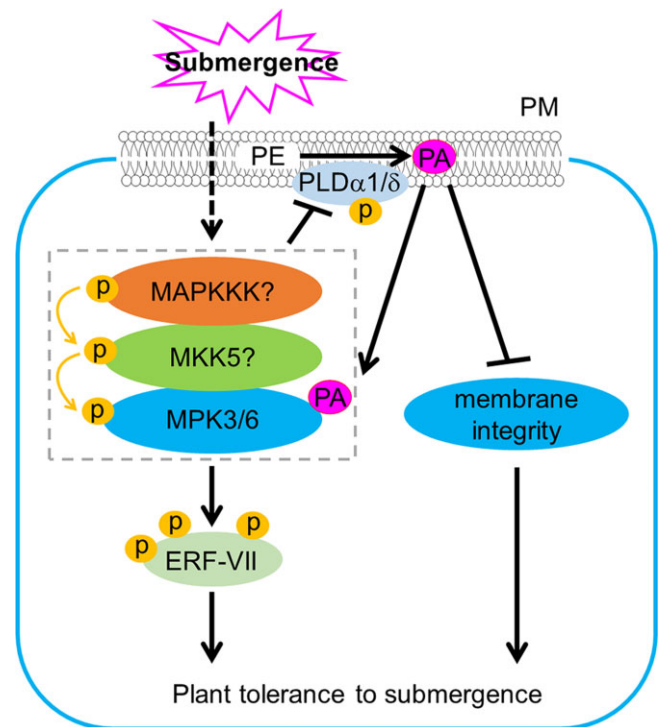


Figure 8 A working model of the role of PLDs and PA in plant responses to submergence-induced hypoxia. Submergence activates the two PLDs, PLD α 1 and PLD δ , which results in PA production. PA then acts as a signaling molecule, enhancing the activities of MPK3 and MPK6 and thus regulating ERF-VII-mediated hypoxia signaling. However, accumulation of PA also leads to higher levels of ROS, cell death, and destruction of membrane integrity under long-term submergence. MPK3 and MPK6 regulate PLD α 1 and PLD δ protein levels through a regulatory feedback mechanism to inhibit PA production, thus maintaining PA content and cellular homeostasis at an appropriate level under hypoxia.

mammalian cells, the protein kinase C α phosphorylates PLD1 and in turn suppresses its activity (Hu and Exton, 2003), indicating that this regulatory mechanism may be conserved across animal and plant species.

In summary, our observations present strong evidence to support the dual roles of PA in the regulation of membrane integrity and the MPK3/6–RAP2.12 module in plant responses to submergence (Figure 8). Submergence activates PLD α 1 and PLD δ to hydrolyze PE for generating PA (Figure 8; Xie et al., 2015a). Furthermore, PA binds to MPK3 and MPK6 proteins and enhances their activities; in turn, these kinases phosphorylate ERF-VII-type transcription factors, such as RAP2.12, to promote their transcriptional activity (Figure 8), which may represent a key step in stimulating hypoxia signaling. At the same time, the accumulation of PA leads to enhanced ROS levels, premature cell death, and destruction of membrane integrity, which negatively affects plant survival upon recovery from submergence (Figure 8). Thus, the MPK3 and MPK6 kinases form a regulatory feedback loop with PLD α 1 and PLD δ to reduce their protein levels, thus serving as a protective mechanism for maintaining

PA at proper physiological levels under long-term hypoxia conditions.

Materials and methods

Plant materials and growth conditions

All WT and mutant *Arabidopsis* (*A. thaliana*) plants used in this study were in the Columbia-0 (Col-0) background. The T-DNA insertional mutants of *PLD α 1* (At3g15730), *PLD δ* (At4g35790), *MPK3* (At3g45640), and *MPK6* (At2g43790) were identified from The Arabidopsis Information Resource website (<http://www.arabidopsis.org>) and are referred to as *pld α 1* (SALK_053785), *pld δ* (SALK_023247), *mpk3* (CS466883), and *mpk6* (SALK_062471C), respectively. The *mpk3 mpk6-es* line (estradiol-inducible silencing of *MPK3* by RNA interference in the *mpk6* mutant background) was described previously (Cheng et al., 2015). The *pld α 1*, *pld δ* , *mpk3*, and *mpk6* mutants were crossed to generate *pld α 1 pld δ* , *pld α 1 mpk3*, *pld α 1 mpk6*, *pld δ mpk3*, and *pld δ mpk6* double mutants. The RAP2.12-GFP transgenic lines were generated as described previously (Zhou et al., 2020). The primers used to genotype all mutants are listed in [Supplemental Data Set S1](#).

All seeds were surface-sterilized with 20% bleach containing 0.1% Tween-20 for 15 min followed by at least five washes with sterile water. Seeds were then sown on half-strength MS medium (Sigma-Aldrich, St Louis, MO, USA) with 1% sucrose, 0.8% agar, and adjusted to pH 5.8, and stratified for 3 days in the dark at 4°C. After germination for 7 days, seedlings were transplanted to soil and grown in a plant growth room with a 16-h light (170 $\mu\text{mol m}^{-2} \text{s}^{-1}$ using Philips F17T8/TL841 17W bulbs)/8-h dark photoperiod at 22°C.

Plasmid construction

All plasmids used in this study were generated using an In-Fusion method. Primers for all constructs are listed in [Supplemental Data Set S1](#). To generate constructs for transient expression, the full-length coding regions of *MPK3*, *MPK6*, and *RAP2.12* were inserted into BamHI- and StuI-digested pUC119 plasmids to obtain *MPK3-HA*, *MPK6-HA*, *RAP2.12-HA*, *MPK3-FLAG*, and *MPK6-FLAG* constructs. Similarly, full-length coding regions of *PLD α 1* and *PLD δ* sequences were cloned into BamHI- and PstI-digested pUC119 to generate *FLAG-PLD α 1* and *FLAG-PLD δ* constructs. To generate plasmids for BiFC analysis, full-length coding sequence fragments of *MPK3*, *MPK6*, *MPK9*, *CPK12*, *PLD α 1*, and *PLD δ* were amplified and inserted into pHBT-YN or pHBT-YC vectors digested by BamHI. To generate plasmids for recombinant protein expression, the vectors pGEX6p-1 and pMAL-MBP-His were used. The full-length coding regions of *MPK3*, *MPK6*, *RAP2.12*, *PLD α 1*, *PLD δ* , *ERF6*, and *ACBP1* were inserted into BamHI-digested pGEX6p-1 plasmids, and the full-length coding regions of *MPK3*, *MPK6*, and *MKK5^{DD}* were inserted into BamHI-digested pMAL-MBP-His plasmids.

Treatments

For hypoxia germination assays, following stratification for 3 days, seeds sown on half-strength MS medium were transferred to an enclosed hypoxic workstation (Anaerobic System model 1025; Forma Scientific, <http://www.thermo.com>) with 3% O₂ and a 16-h light (125 $\mu\text{mol m}^{-2} \text{s}^{-1}$)/8-h dark photoperiod at 22°C for 10 days. Plates were photographed and the proportion of seedlings with green cotyledons was calculated.

For hypoxia-induced leaf damage assays, 6-day-old seedlings were transferred onto half-strength MS plates without sucrose. Seedlings were treated in a hypoxia workstation with 0.1% O₂ in the dark for 5 days and allowed to recover in a growth room for 3 days under normal light/dark conditions.

Submergence treatments were carried out as described previously (Xie et al., 2015b). Briefly, 4-week-old plants were submerged to a final depth of 5–10 cm beneath the water surface for 8 days under normal light–dark conditions. Plant samples were photographed after 3 days of recovery. Dry weights and survival rates were recorded after 7 days of recovery. Aboveground *Arabidopsis* tissues were harvested, heated overnight to 65°C to dry, and weighed again to obtain dry weights. The survival rates were calculated based on the numbers of plants that produced new leaves and continued to grow after recovery from submergence.

For hypoxia germination assays, seeds of the WT, *mpk3*, *mpk6*, and *mpk3 mpk6-es* line sown on half-strength MS medium containing 10 μM estradiol (Sigma, 50 mM stock in DMSO), were transferred to an enclosed hypoxic workstation (3% O₂). Similarly, 6-day-old WT, *mpk3*, *mpk6*, and *mpk3 mpk6-es* seedlings grown on half-strength MS medium were transferred onto half-strength MS plates containing 10 μM estradiol, and placed into an enclosed hypoxic workstation (0.1% O₂). For submergence treatments, 4-week-old adult plants of the WT, *mpk3*, *mpk6*, and *mpk3 mpk6-es* grown under normal growth conditions were sprayed with 10 μM estradiol for 3 days before submergence.

For phospholipid treatments, liposomes were produced according to Zhang et al. (2009) with minor revisions. Briefly, natural lipid mixtures purified from soybean (*Glycine max*) (PA [Cat #840074], PC [Cat #441601], PE [Cat #840024], PS [Cat #870336]; Avanti Polar Lipids; stored at –20°C in the dark) were dissolved in chloroform and dried under nitrogen flow. The lipid films were rehydrated in ice-cold optimized buffer (50 mM Tris–HCl pH 7.4, 150 mM NaCl, 10 mM MgCl₂, 0.05% [v/v] Tween-20) and then processed by five cycles of 10-s sonication, generating a final liposome concentration of 50 μM . An equal volume of chloroform was processed in the same manner and used as mock control. The detached leaves of 3-week-old *RAP2.12-GFP* transgenic plants were treated with 50 μM liposomes prepared from PA, PC, PE, or PS for 3 h. The leaves similarly treated with dilution buffer were set as mock controls. GFP fluorescence was detected at 488 nm by confocal microscopy.

Lipid profiling

Total lipid extraction was performed as described previously (Welti et al., 2002; Xie et al., 2015a). Briefly, Arabidopsis leaves were immersed in isopropanol preheated to 75°C with 0.01% butylated hydroxytoluene (phospholipase inhibitor) immediately after sampling and incubated at 75°C for another 15 min to inhibit lipolytic enzymes, particularly PLD, in plant tissues (Welti et al., 2002). The profiles of membrane lipids were determined by automated electrospray ionization–tandem mass spectrometry as previously described (Devaiah et al., 2006). Extracts were dried under nitrogen flow, dissolved in 1 mL of chloroform, and analyzed on a triple TOF 5600 MS/MS system (AB SCIEX, Vaughan, Canada). Separations were accomplished on a Phenomenex Kinetex C18 column (150 × 2.1 mm, 2.6 μm). Phospholipid standards were purchased from Avanti Polar Lipids. Quantification was performed by normalizing the peak areas to the internal standards.

Measurement of electrolyte leakage and water loss

Electrolyte leakage was measured as previously described (Chen et al., 2015). Briefly, ion leakage was measured using a conductivity meter (Mettler Toledo S220-USP/EP). Conductivity was measured from the water used to soak excised whole leaves with gentle shaking at room temperature for 1 h. Subsequently, the solution (with leaves) was heated to 100°C in a water bath for 10 min and cooled down to room temperature to determine total ion strength. Ion leakage values were calculated by comparing leaked ion strength to the corresponding total ion strength.

Water loss was determined following Zhang et al. (2012). Arabidopsis rosettes were collected after submergence, placed in empty Petri dishes under normal conditions and weighed every 20 min for 2 h. Relative loss of fresh weight (%) was used to represent water loss.

Measurement of H₂O₂ and MDA

H₂O₂ contents were measured using the Amplex Red H₂O₂/Peroxidase Assay Kit (Molecular Probes, Eugene, OR, USA) according to Pucciariello et al. (2012). In brief, 30 mg of rosettes was ground to a fine powder in liquid nitrogen and dissolved in 200 μL of reaction buffer. After centrifugation at 12,000 g for 10 min at 4°C, 50 μL of supernatant was mixed with 50 μL of the 3% H₂O₂ working solution provided by the kit, followed by incubation for 30 min at room temperature in the dark. Absorbance was measured at 560 nm with a microplate reader (Tecan, Männedorf, Switzerland). H₂O₂ concentration was determined using a standard curve, according to the manufacturer's instructions.

MDA levels were determined with the Lipid Peroxidation MDA Assay Kit (Beyotime, Shanghai, China) with minor modifications. Briefly, leaves were homogenized in 150 μL buffer (10 mM 4-(2-hydroxyethyl)-1-piperazineethanesulfonic acid (HEPES) pH 7.4, 150 mM NaCl, 2 mM EDTA, and 10% [v/v] glycerol) followed by centrifugation at 12,000 g for 10 min at 4°C. Then, 100 μL of supernatant was mixed with 200-μL MDA working solution supplied with the kit. After

boiling at 100°C for 15 min, the mixtures were quickly cooled down on ice, followed by centrifugation at 12,000 g for 10 min at 4°C. Absorbance was recorded at 532 nm using a microplate reader (Tecan). MDA concentrations were determined using a standard curve following the manufacturer's instructions.

Total RNA extraction and real-time quantitative PCR (qPCR) analysis

Total RNA was extracted with the HiPure plant RNA mini kit and reverse-transcribed using the HiScript II Q RT SuperMix kit with gDNA Wiper (Vazyme, Nanjing, China) according to the manufacturer's instructions. qPCR was performed using the ChamQ SYBR color qPCR master mix (Vazyme) on a StepOne Plus Real-Time PCR system (Applied Biosystems, Waltham, MA, USA). ACTIN2 was used as the reference gene for normalization. Three technical replicates were performed for each sample. Gene-specific primers for qPCR analysis are listed in Supplemental Data Set S1.

Protein extraction and immunoblot analysis

For total protein extraction, Arabidopsis samples were ground in liquid nitrogen and homogenized in ice-cold extraction buffer (50-mM sodium phosphate, pH 7.0, 200-mM NaCl, 10-mM MgCl₂, 0.2% [v/v] β-mercaptoethanol, and 10% [v/v] glycerol) containing 1 × protease inhibitor cocktail (Roche Basel, Switzerland; 04693132001). The samples were incubated on ice for 30 min and centrifuged for 30 min at 12,000 g at 4°C. The supernatant was transferred to a new microcentrifuge tube for electrophoresis.

For immunoblot analysis, total proteins were subjected to SDS–PAGE and transferred to a Hybond-C membrane (Amersham Biosciences, Amersham, UK). Anti-HA (Sigma-Aldrich; cat. No. H6533, 1:5,000), anti-FLAG (Sigma-Aldrich; cat. No. A8592, 1:5,000), anti-GST (Abcam, Cambridge, UK; ab3416, 1:5,000), anti-His (Cell Signaling Technology, Danvers, MA, USA; cat. No. 2366, 1:3,000), anti-PLDα1 (Agrisera, Vaesterbotten, Sweden; cat. No. AS09558, 1:1,000), anti-MPK3 (Agrisera; cat. No. AS164024, 1:1,000), anti-MPK6 (Agrisera; cat. No. AS122633, 1:1,000), anti-phospho-p44/42-ERK (anti-pTEpY) (Cell Signaling Technology; cat. No. 9101, 1:1,000), Anti-Thiophosphate ester (Abcam; ab92570, 1:5,000), and anti-Plant Actin (Abbkine, Wuhan, China; cat. No. A01050, 1:5,000) antibodies were used for immunoblotting.

For in vivo MPK3 and MPK6 phosphorylation activity assays, 10-day-old WT seedlings grown on solid MS medium were then transferred to liquid MS medium containing 50 μM liposomes of PA or PS (natural lipid mixtures purified from soy; Avanti Polar Lipids), and harvested at the indicated times. Total proteins were extracted for immunoblot analyses using specific antibodies.

In vitro lipid–protein binding and pull-down assays

Lipid–protein membrane binding assays were performed as described previously (Xiao et al., 2010). Briefly, recombinant GST-MPK3 and GST-MPK6 proteins were produced in

Escherichia coli and purified using glutathione beads (GE Healthcare, Chicago, IL, USA). Various natural lipid mixtures purified from soy (PA, PC, PE, PI [Cat #840044], PG [Cat #841148], and PS; Avanti Polar Lipids; 50 μ M) were spotted onto nitrocellulose membranes, followed by incubation at room temperature for 1 h in the dark. The lipid-bound membrane was blocked in Tris-buffered saline (TBS) with 1% (w/v) nonfat milk for 1 h and then incubated with 5 μ g GST, GST-MPK3 or GST-MPK6, respectively, in blocking buffer for 3 h at 4°C. The membrane was then gently washed 3 times for 10 min each with TBST (TBS plus 0.1% Tween-20). After incubation with the GST antibodies for 2 h at room temperature, the filter was again washed 3 times for 10 min each with TBST. Proteins were detected by immunoblotting with anti-GST antibody as described above.

For the protein-PA binding assays on beads, 10 μ g of recombinant GST-MPK3, GST-MPK6, GST-PYL4, or GST, was diluted in 500 μ L binding buffer (10 mM HEPES, pH 7.4, 150 mM NaCl, 0.25% [v/v] Igepal), to which 50 μ L of PA beads or PI beads were added, followed by incubation for 3 h at 4°C. After three washes with wash buffer (10 mM HEPES, pH 7.4, 150 mM NaCl, 0.25% [v/v] Igepal), the beads were detected by immunoblotting with anti-GST antibody.

MST assay

For MST analysis, protein labeling was performed with reactive dyes using the Monolith NT Protein Labeling Kit RED (Mo-L011). The concentration of labeled proteins was adjusted to 10 nM using the labeling buffer 1 \times phosphate buffer saline (pH 7.6) containing 0.05% (v/v) Tween-20. A serial dilution of various liposomes of PA, PC, PI, and PS (natural lipid mixtures purified from soy; Avanti Polar Lipids) ranging from 1.5 nM to 50 μ M was prepared for mixing with the labeled proteins, followed by incubation for 5 min in the dark. The combined solutions of labeled proteins and liposomes were filled into standard treated capillaries via capillary force. Fluorescence scans were carried out on a Nano Temper Monolith NT.115 (40% LED power; 50% laser power), to determine binding affinities.

Co-IP and BiFC assays

Plasmids for transient transfection were extracted from the relevant *E. coli* cultures using a Maxi Kit (Omega, Bienne, Switzerland; D6922-02). Arabidopsis mesophyll protoplasts were prepared and transfected as described previously by Yoo et al. (2007). Protoplasts were isolated from the rosettes of 4-week-old plants and transfected with the indicated plasmids, followed by culture for 16 h to allow protein accumulation. For Co-IP assays, total proteins were extracted with IP buffer (10-mM HEPES, pH 7.4, 150-mM NaCl, 2-mM EDTA, and 10% [v/v] glycerol) with 0.25% (v/v) Triton X-100. A portion of the total lysate (10%) was set aside as input, while the remaining supernatant was incubated with anti-FLAG beads or anti-HA beads for 4 h at 4°C. Beads were washed 5 times with IP buffer containing 0.1% (v/v) Triton X-100, followed by elution in IP buffer at 95°C for 5 min before immunoblot analysis.

For BiFC assays, the pairs of split nYFP and cYFP plasmids MPK3-nYFP/PLD α 1-cYFP, MPK6-nYFP/PLD α 1-cYFP, MPK3-nYFP/PLD δ -cYFP, MPK6-nYFP/PLD δ -cYFP, CPK12-nYFP/PLD α 1-cYFP, MPK9-nYFP/PLD δ -cYFP, or nYFP/cYFP were co-transfected into leaf protoplasts. Fluorescence was detected after incubation for 16 h under normal conditions by confocal microscopy.

Phosphorylation assays

In vitro phosphorylation assays were performed as described previously (Hertz et al., 2010). Recombinant GST-MPK3, GST-MPK6, MBP-MPK3-His, MBP-MPK6-His, or MBP-MKK5^{DD}-His (0.5 μ g) were incubated with the substrate proteins GST-PLD α 1 or GST-PLD δ , GST-RAP2.12 or GST-RAP2.12^{6A} (1 μ g), respectively, in reaction buffer (20-mM HEPES pH 7.4, 0.15 M NaCl, 10 mM MgCl₂ and 3 μ L of 10 mM N⁶-substituted ATP γ S) at room temperature for 30 min, then supplemented with 1.5 μ L of 50 mM PNBM at room temperature for 1 h. The reactions were stopped by the addition of 5 \times SDS sample buffer. Phosphorylated substrate proteins were detected with a thiophosphate ester-specific antibody (Abcam; ab92570, 1:5,000) after separation by 10% SDS-PAGE.

To detect the specific effect of PA on MKK5-MPK6-mediated phosphorylation of RAP2.12, recombinant MBP-MPK6-His and MBP-MKK5^{DD}-His (0.5 μ g) were incubated in reaction buffer (20 mM HEPES pH 7.4, 0.15 M NaCl, 10 mM MgCl₂, and 3 μ L of 10 mM unlabeled ATP) at room temperature for 1 h to ensure prior phosphorylation and activation of MPK6 by MKK5^{DD}. Subsequently, GST-RAP2.12 protein, 3 μ L of 10 mM N⁶-substituted ATP γ S, and 50 μ M PA (natural lipid mixture purified from soy; Avanti Polar Lipids) liposomes were added to the reaction and incubated for another 30 min at room temperature. The reaction was then supplemented with 1.5 μ L of 50 mM PNBM and incubated at room temperature for 1 h.

For in vivo dephosphorylation assays, protoplasts were prepared from 4-week-old WT plants and the relevant plasmids were co-transfected as above. After a 16-h incubation, proteins were extracted from transfected protoplasts in IP buffer (10 mM HEPES [pH 7.4], 150 mM NaCl, 2 mM EDTA, and 10% [v/v] glycerol) with 0.25% (v/v) Triton X-100 and Protease inhibitor cocktails (Roche). An aliquot of each extract was then incubated with λ -PPase (New England Biolabs, Ipswich, MA, USA), and 1 \times phosphatase inhibitor (Roche) at 30°C for 30 min. The reaction mixtures were terminated by adding 5 \times SDS loading buffer and boiling at 95°C for 5 min. Immunoblot analyses were performed with anti-FLAG and anti-HA antibodies.

Measurement of LUC activity

All reporter constructs used in this study were generated in the pGreen II 0800-LUC vector according to Hellens et al. (2005), and the effector constructs were generated using the pUC119 construct driven by the *UBQ10* promoter. The primers for all constructs are listed in Supplemental Data Set S1. WT or *pld α 1* *pld δ* protoplasts were prepared and

transfected as described previously (Yoo et al., 2007). Firefly LUC and Renilla LUC (REN) activities were determined using the Dual-LUC Reporter Assay System (Promega, Madison, WI, USA) and the SpectraMax i3x Multi-Mode detection Platform (Molecular Devices). Relative LUC activity was expressed as the ratio of LUC activity to REN activity.

Identification of in vivo phosphorylation sites by mass spectrometry

To identify the phosphorylation sites of PLD α 1, frozen tissues from 2-week-old UBQ10_{pro}:FLAG-PLD α 1 transgenic seedlings (10 g fresh weight) were ground in a chilled mortar. After addition of 10 mL IP buffer (10 mM HEPES, pH 7.4, 150 mM NaCl, 2 mM EDTA, and 10% [v/v] glycerol) with 0.1% (v/v) Triton X-100, phosphatase inhibitor cocktails, and protease inhibitor cocktail (Roche), the crude extract was placed on ice for 30 min and centrifuged at 10,000g for 30 min at 4°C twice. The supernatant was subsequently transferred to a new microcentrifuge tube, and incubated with 100 μ L anti-FLAG beads at 4°C overnight. Beads were then washed 10–20 times using IP buffer containing 0.2% (v/v) Triton X-100, followed by elution in IP buffer at 95°C for 5 min before immunoblot analysis. The protein band corresponding to PLD α 1 was visualized by Coomassie brilliant blue staining and the gel slice was subjected to mass spectrometric analysis at the APTBIO company (Shanghai, China).

Statistical analysis

Data reported in this study are means \pm SD of three independent experiments unless otherwise indicated. The significance of the differences between groups was determined by a two-tailed Student's *t* test (Supplemental Data Set S2). *P* < 0.05 or < 0.01 were considered significant. The relative intensities of each band on immunoblots were quantified using ImageJ.

Accession numbers

Sequence data used in this article can be found in the Arabidopsis Genome Initiative database under the following accession numbers: PLD α 1 (AT3G15730), PLD δ (AT4G35790), RAP2.12 (AT1G53910), MPK3 (AT3G45640), MPK6 (AT2G43790), MKK5 (AT3G21220), MPK9 (AT3G18040), CPK12 (AT5G23580), DGK1 (AT5G07920), DGK5 (AT2G20900), ADH1 (AT1G77120), PYL4 (AT2G38310), ERF6 (AT4G17490), and ACBP1 (AT5G53470).

Supplemental data

The following materials are available in the online version of this article.

Supplemental Figure S1. RT-qPCR analysis showing the expression of PLDs and DGKs in response to submergence.

Supplemental Figure S2. Characterization of T-DNA insertional mutants in PLD α 1 and PLD δ .

Supplemental Figure S3. PLD α 1/ δ -mediated submergence tolerance is related to H₂O₂ production and MDA contents.

Supplemental Figure S4. Recombinant MPK3 and MPK6 proteins bind PA in vitro.

Supplemental Figure S5. Characterization of the *mpk3*, *mpk6* single mutants, and the *mpk3 mpk6-es* line.

Supplemental Figure S6. Schematic diagrams of effector and reporter constructs used in LUC assays.

Supplemental Figure S7. MPK3 and MPK6 phosphorylate RAP2.12 in vitro.

Supplemental Figure S8. Identification of phosphorylation sites in the RAP2.12 protein.

Supplemental Figure S9. Controls for the BiFC assay of PLD α 1 or PLD δ and CPK12 or MPK9 in Arabidopsis.

Supplemental Figure S10. Identification of PLD α 1 phosphorylation sites.

Supplemental Figure S11. PC and PE contents in WT and *mpk3,6-es* plants in response to submergence.

Supplemental Data Set S1. Primers used in this study.

Supplemental Data Set S2. Details of the *t* test analysis in this study.

Acknowledgments

We thank the ABRC (www.arabidopsis.org) for providing *pld α 1*, *pld δ* , *mpk3*, and *mpk6* mutant seed pools, and Dr Pengcheng Wang (Shanghai Center for Plant Stress Biology, Chinese Academy of Sciences, China) for providing MKK5^{DD} construct.

Funding

This work was supported by the National Natural Science Foundation of China (Projects 31725004, 31970298, and 32000215), Key Realm R&D Program of Guangdong Province (Project 2020B0202090001), the Natural Science Foundation of Guangdong Province (Projects 2017A030308008, 2019A1515012155, and 2018A030313210), China Postdoctoral Science Foundation (2021M690172), and Sun Yat-sen University (Project 33000-31143406).

Conflict of interest statement. None declared.

References

- Arisz SA, Testerink C, Munnik T (2009) Plant PA signaling via diacylglycerol kinase. *Biochim Biophys Acta* **1791**: 869–875
- Arisz SA, van Wijk R, Roels W, Zhu JK, Haring MA, Munnik T (2013) Rapid phosphatidic acid accumulation in response to low temperature stress in Arabidopsis is generated through diacylglycerol kinase. *Front Plant Sci* **4**: 1
- Bailey-Serres J, Voisenek LA (2008) Flooding stress: acclimations and genetic diversity. *Annu Rev Plant Biol* **59**: 313–339
- Bargmann BOR, Laxalt AM, ter Riet B, van Schooten B, Merquiol E, Testerink C, Haring MA, Bartels D, Munnik T (2009a) Multiple PLDs required for high salinity and water deficit tolerance in plants. *Plant Cell Physiol* **50**: 78–89
- Bargmann BO, Laxalt AM, ter Riet B, Testerink C, Merquiol E, Mosblech A, Leon-Reyes A, Pieterse CM, Haring MA, Heilmann

- I, et al. (2009b) Reassessing the role of phospholipase D in the Arabidopsis wounding response. *Plant Cell Environ* **32**: 837–850
- Chang R, Jang CJH, Branco-Price C, Nghiem P, Bailey-Serres J** (2012) Transient MPK6 activation in response to oxygen deprivation and reoxygenation is mediated by mitochondria and aids seedling survival in Arabidopsis. *Plant Mol Biol* **78**: 109–122
- Chen L, Liao B, Qi H, Xie LJ, Huang L, Tan WJ, Zhai N, Yuan LB, Zhou Y, Yu LJ, et al.** (2015) Autophagy contributes to regulation of the hypoxia response during submergence in *Arabidopsis thaliana*. *Autophagy* **11**: 2233–2246
- Cheng Z, Li JF, Niu Y, Zhang XC, Woody OZ, Xiong Y, Djonović S, Millet Y, Bush J, McConkey BJ, et al.** (2015) Pathogen-secreted proteases activate a novel plant immune pathway. *Nature* **521**: 213–216
- Cho HY, Wen TN, Wang YT, Shih MC** (2016) Quantitative phosphoproteomics of protein kinase SnRK1 regulated protein phosphorylation in Arabidopsis under submergence. *J Exp Bot* **67**: 2745–2760
- Colcombet J, Hirt H** (2008) Arabidopsis MAPKs: a complex signalling network involved in multiple biological processes. *Biochem J* **413**: 217–226
- Cruz-Ramírez A, Oropeza-Aburto A, Razo-Hernández F, Ramírez-Chávez E, Herrera Estrella L** (2006) Phospholipase D22 plays an important role in extraplastidic galactolipid biosynthesis and phosphate recycling in Arabidopsis roots. *Proc Natl Acad Sci USA* **103**: 6765–6770
- Devaiah SP, Roth MR, Baughman E, Li M, Tamura P, Jeannotte R, Welti R, Wang X** (2006) Quantitative profiling of polar glycerolipid species from organs of wild-type Arabidopsis and a PHOSPHOLIPASE D α 1 knockout mutant. *Phytochemistry* **67**: 1907–1924
- Dubots E, Audry M, Yamaryo Y, Bastien O, Ohta H, Breton C, Maréchal E, Block MA** (2010) Activation of the chloroplast monogalactosyl diacylglycerol synthase MGD1 by phosphatidic acid and phosphatidylglycerol. *J Biol Chem* **285**: 6003–6011
- Fukao T, Xu K, Ronald PC, Bailey-Serres J** (2006) A variable cluster of ethylene response factor-like genes regulates metabolic and developmental acclimation responses to submergence in rice. *Plant Cell* **18**: 2021–2034
- Gibbs DJ, Lee SC, Isa NM, Gramuglia S, Fukao T, Bassel GW, Correia CS, Corbineau F, Theodoulou FL, Bailey-Serres J, et al.** (2011) Homeostatic response to hypoxia is regulated by the N-end rule pathway in plants. *Nature* **479**: 415–418
- Gómez-Merino FC, Brearley CA, Ornatowska M, Abdel-Halim ME, Zanor MI, Mueller-Roeber B** (2004) AtDGK2, a novel diacylglycerol kinase from *Arabidopsis thaliana*, phosphorylates 1-stearoyl-2-arachidonoyl-sn-glycerol and 1,2-dioleoyl-sn-glycerol and exhibits cold-inducible gene expression. *J Biol Chem* **279**: 8230–8241
- Guo L, Mishra G, Taylor K, Wang X** (2011) Phosphatidic acid binds and stimulates Arabidopsis sphingosine kinases. *J Biol Chem* **286**: 13336–13345
- Hellens RP, Allan AC, Friel EN, Bolitho K, Grafton K, Templeton MD, Karunaitnam S, Gleave AP, Laing WA** (2005) Transient expression vectors for functional genomics, quantification of promoter activity and RNA silencing in plants. *Plant Methods* **1**: 13
- Hertz NT, Wang BT, Allen JJ, Zhang C, Dar AC, Burlingame AL, Shokat KM** (2010) Chemical genetic approach for kinase-substrate mapping by covalent capture of thiophosphopeptides and analysis by mass spectrometry. *Curr Protocol Chem Biol* **2**: 15–36
- Hong YY, Zhang WH, Wang XM** (2010) Phospholipase D and phosphatidic acid signalling in plant response to drought and salinity. *Plant Cell Environ* **33**: 627–635
- Hu T, Exton JH** (2003) Mechanisms of regulation of phospholipase D1 by protein kinase C alpha. *J Biol Chem* **278**: 2348–2355
- Hyodo K, Taniguchi T, Manabe Y, Kaido M, Mise K, Sugawara T, Taniguchi H, Okuno T** (2015) Phosphatidic acid produced by phospholipase D promotes RNA replication of a plant RNA virus. *PLoS Pathog* **11**: e1004909
- Katagiri T, Takahashi S, Shinozaki K** (2001) Involvement of a novel Arabidopsis phospholipase D, AtPLD δ , in dehydration-inducible accumulation of phosphatidic acid in stress signalling. *Plant J* **26**: 595–605
- Kim H, Choi D, Suh MC** (2017) Cuticle ultrastructure, cuticular lipid composition, and gene expression in hypoxia-stressed Arabidopsis stems and leaves. *Plant Cell Rep* **36**: 815–827
- Kuiper PJC** (1970) Lipids in alfalfa leaves in relation to cold hardiness. *Plant Physiol* **45**: 684–686
- Li W, Li M, Zhang W, Welti R, Wang X** (2004) The plasma membrane-bound phospholipase D δ enhances freezing tolerance in *Arabidopsis thaliana*. *Nat Biotechnol* **22**: 427–433
- Li W, Song T, Wallrad L, Kudla J, Wang X, Zhang W** (2019) Tissue-specific accumulation of pH-sensing phosphatidic acid determines plant stress tolerance. *Nat Plants* **5**: 1012–1021
- Li-Beisson Y, Shorrosh B, Beisson F, Andersson MP, Arondel V, Bates PD, Baud S, Bird D, Debono A, Durrett TX, et al.** (2013) Acyl-lipid metabolism. *Arabidopsis Book* **11**: e0161
- Licausi F, Kosmacz M, Weits DA, Giuntoli B, Giorgi FM, Voeselek LACJ, Perata P, van Dongen JT** (2011) Oxygen sensing in plants is mediated by an N-end rule pathway for protein destabilization. *Nature* **479**: 419–422
- McLoughlin F, Testerink C** (2013) Phosphatidic acid, a versatile water-stress signal in roots. *Front Plant Sci* **4**: 525
- Meng X, Xu J, He Y, Yang KY, Mordorski B, Liu Y, Zhang S** (2013) Phosphorylation of an ERF transcription factor by Arabidopsis MPK3/MPK6 regulates plant defense gene induction and fungal resistance. *Plant Cell* **25**: 1126–1142
- Meng XZ, Zhang SQ** (2013) MAPK cascades in plant disease resistance signaling. *Annu Rev Phytopathol* **51**: 245–266
- Mishra G, Zhang W, Deng F, Zhao J, Wang X** (2006) A bifurcating pathway directs abscisic acid effects on stomatal closure and opening in Arabidopsis. *Science* **312**: 264–276
- Moellering ER, Benning C** (2011) Galactoglycerolipid metabolism under stress: a time for remodeling. *Trends Plant Sci* **16**: 98–107
- Moellering ER, Muthan B, Benning C** (2010) Freezing tolerance in plants requires lipid remodeling at the outer chloroplast membrane. *Science* **330**: 226–228
- Pinosa F, Buhot N, Kwaaitaal M, Fahlberg P, Thordal-Christensen H, Ellerström M, Andersson MX** (2013) Arabidopsis phospholipase D δ is involved in basal defense and nonhost resistance to powdery mildew fungi. *Plant Physiol* **163**: 896–906
- Pucciariello C, Parlanti S, Banti V, Novi G, Perata P** (2012) Reactive oxygen species-driven transcription in Arabidopsis under oxygen deprivation. *Plant Physiol* **159**: 184–196
- Qin C, Wang C, Wang X** (2002) Kinetic analysis of Arabidopsis phospholipase Ddelta. Substrate preference and mechanism of activation by Ca²⁺ and phosphatidylinositol 4,5-bisphosphate. *J Biol Chem* **277**: 49685–49690
- Rajashekar CB, Zhou HE, Zhang Y, Li W, Wang X** (2006) Suppression of phospholipase Dalpha1 induces freezing tolerance in Arabidopsis: response of cold-responsive genes and osmolyte accumulation. *J Plant Physiol* **163**: 916–926
- Rodriguez MC, Petersen M, Mundy J** (2010) Mitogen-activated protein kinase signaling in plants. *Annu Rev Plant Biol* **61**: 621–664
- Sasidharan R, Mustruph A** (2011) Plant oxygen sensing is mediated by the N-end rule pathway: a milestone in plant anaerobiosis. *Plant Cell* **23**: 4173–4183
- Sasidharan R, Hartman S, Liu Z, Martopawiro S, Sajeev N, van Veen H, Yeung E, Voeselek LACJ** (2018) Signal dynamics and interactions during flooding stress. *Plant Physiol* **176**: 1106–1117
- Schmidt RR, Weits DA, Feulner CFJ, van Dongen JT** (2018) Oxygen sensing and integrative stress signaling in plants. *Plant Physiol* **176**: 1131–1142
- Singh P, Sinha AK** (2016) A positive feedback loop governed by SUB1A1 interaction with MITOGEN-ACTIVATED PROTEIN KINASE3 imparts submergence tolerance in rice. *Plant Cell* **28**: 1127–1143

- Tan WJ, Yang YC, Zhou Y, Huang LP, Xu L, Chen QF, Yu LJ, Xiao S (2018) DIACYLGLYCEROL ACYLTRANSFERASE and DIACYLGLYCEROL KINASE modulate triacylglycerol and phosphatidic acid production in the plant response to freezing stress. *Plant Physiol* **177**: 1303–1318
- Testerink C, Larsen PB, van der Does D, van Himbergen JA, Munnik T (2007) Phosphatidic acid binds to and inhibits the activity of Arabidopsis CTR1. *J Exp Bot* **58**: 3905–3914
- Thomashow MF (1999) Plant cold acclimation: freezing tolerance genes and regulatory mechanisms. *Annu Rev Plant Physiol Plant Mol Biol* **50**: 571–599
- Uraji M, Katagiri T, Okuma E, Ye WX, Hossain MA, Masuda C, Miura A, Nakamura Y, Mori IC, Shinozaki K, et al. (2012) Cooperative function of PLD δ and PLD α 1 in abscisic acid-induced stomatal closure in Arabidopsis. *Plant Physiol* **159**: 450–460
- Vadović P, Šamajová O, Takáč T, Novák D, Zapletalová V, Colcombet J, Šamaj J (2019) Biochemical and genetic interactions of phospholipase D alpha 1 and mitogen-activated protein kinase 3 affect Arabidopsis stress response. *Front Plant Sci* **10**: 275
- Verkleij AJ, De Maagd R, Leunissen-Bijvelt J, De Kruijff B (1982) Divalent cations and chlorpromazine can induce non-bilayer structures in phosphatidic acid-containing model membranes. *Biochim Biophys Acta* **684**: 255–262
- Wang M, Shen Y, Tao F, Yang S, Li W (2016) Submergence induced changes of molecular species in membrane lipids in *Arabidopsis thaliana*. *Plant Divers* **38**: 156–162
- Wang X (2005) Regulatory functions of phospholipase D and phosphatidic acid in plant growth, development, and stress responses. *Plant Physiol* **139**: 566–573
- Wang X, Devaiah SP, Zhang W, Welti R (2006) Signaling functions of phosphatidic acid. *Prog Lipid Res* **45**: 250–278
- Wang X, Su Y, Liu Y, Kim SC, Fanella B (2014) Signaling and Communication in Plants. Springer, New York, NY
- Welti R, Li W, Li M, Sang Y, Biesiada H, Zhou HE, Rajashekar CB, Williams TD, Wang X (2002) Profiling membrane lipids in plant stress responses. Role of phospholipase D alpha 1 in freezing-induced lipid changes in Arabidopsis. *J Biol Chem* **277**: 31994–32002
- Xiao S, Gao W, Chen QF, Chan SW, Zheng SX, Ma J, Wang M, Welti R, Chye ML (2010) Overexpression of Arabidopsis acyl-CoA binding protein ACBP3 promotes starvation-induced and age-dependent leaf senescence. *Plant Cell* **22**: 1463–1482
- Xie LJ, Chen QF, Chen MX, Yu LJ, Huang L, Chen L, Wang FZ, Xia FN, Zhu TR, Wu JX, et al. (2015a) Unsaturation of very-long-chain ceramides protects plant from hypoxia-induced damages by modulating ethylene signaling in Arabidopsis. *PLoS Genet* **11**: e1005143
- Xie LJ, Yu LJ, Chen QF, Wang FZ, Huang L, Xia FN, Zhu TR, Wu JX, Yin J, Liao B, et al. (2015b) Arabidopsis acyl-CoA-binding protein ACBP3 participates in plant response to hypoxia by modulating very-long-chain fatty acid metabolism. *Plant J* **81**: 53–67
- Xie LJ, Tan WJ, Yang YC, Tan YF, Zhou Y, Zhou DM, Xiao S, Chen QF (2020) Long-chain acyl-CoA synthetase LACS2 contributes to submergence tolerance by modulating cuticle permeability in Arabidopsis. *Plants (Basel)* **9**: 262
- Xie LJ, Zhou Y, Chen QF, Xiao S (2021) New insights into the role of lipids in plant hypoxia responses. *Prog Lipid Res* **81**: 101072
- Xu J, Li Y, Wang Y, Liu HX, Lei L, Yang HL, Liu GQ, Ren DT (2008) Activation of MAPK kinase 9 induces ethylene and camalexin biosynthesis and enhances sensitivity to salt stress in Arabidopsis. *J Biol Chem* **283**: 26996–27006
- Xu K, Xu X, Fukao T, Canlas P, Maghirang-Rodriguez R, Heuer S, Ismail AM, Bailey-Serres J, Ronald PC, Mackill DJ (2006) Sub1A is an ethylene-response-factor-like gene that confers submergence tolerance to rice. *Nature* **442**: 705–708
- Xu L, Pan R, Zhou M, Xu Y, Zhang W (2020) Lipid remodelling plays an important role in wheat (*Triticum aestivum*) hypoxia stress. *Funct Plant Biol* **47**: 58–66
- Yao HY, Xue HW (2018) Phosphatidic acid plays key roles regulating plant development and stress responses. *J Integr Plant Biol* **60**: 851–863
- Yoo SD, Cho YH, Sheen J (2007) Arabidopsis mesophyll protoplasts: a versatile cell system for transient gene expression analysis. *Nat Protoc* **2**: 1565–1572
- Yoo SD, Cho YH, Tena G, Xiong Y, Sheen J (2008) Dual control of nuclear EIN3 by bifurcate MAPK cascades in C2 H₄ signalling. *Nature* **451**: 789–795
- Yu L, Nie J, Cao C, Jin Y, Yan M, Wang F, Liu J, Xiao Y, Liang Y, Zhang W (2010) Phosphatidic acid mediates salt stress response by regulation of MPK6 in *Arabidopsis thaliana*. *New Phytol* **188**: 762–773
- Yuan LB, Dai YS, Xie LJ, Yu LJ, Zhou Y, Lai YX, Yang YC, Xu L, Chen QF, Xiao S (2017) Jasmonate regulates plant responses to postsubmergence reoxygenation through transcriptional activation of antioxidant synthesis. *Plant Physiol* **173**: 1864–1880
- Zhang J, Liu H, Sun J, Li B, Zhu Q, Chen S, Zhang H (2012) Arabidopsis fatty acid desaturase FAD2 is required for salt tolerance during seed germination and early seedling growth. *PLoS One* **7**: e30355
- Zhang W, Qin C, Zhao J, Wang X (2004) Phospholipase D α 1-derived phosphatidic acid interacts with ABI1 phosphatase 2C and regulates abscisic acid signaling. *Proc Natl Acad Sci USA* **101**: 9508–9513
- Zhang XD, Wang RP, Zhang FJ, Tao FQ, Li WQ (2013) Lipid profiling and tolerance to low-temperature stress in *Thellungiella salsuginea* in comparison with *Arabidopsis thaliana*. *Biol Plant* **57**: 149–153
- Zhang Y, Zhu H, Zhang Q, Li M, Yan M, Wang R, Wang L, Welti R, Zhang W, Wang X (2009) Phospholipase D α 1 and phosphatidic acid regulate NADPH oxidase activity and production of reactive oxygen species in ABA-mediated stomatal closure in Arabidopsis. *Plant Cell* **21**: 2357–2377
- Zhang Q, Song P, Qu Y, Wang P, Jia Q, Guo L, Zhang C, Mao T, Yuan M, Wang X, et al. (2017) Phospholipase D δ negatively regulates plant thermotolerance by destabilizing cortical microtubules in Arabidopsis. *Plant Cell Environ* **40**: 2220–2235
- Zhao J, Devaiah SP, Wang C, Li M, Welti R, Wang X (2013) Arabidopsis phospholipase D β 1 modulates defense responses to bacterial and fungal pathogens. *New Phytol* **199**: 228–240
- Zhao CZ, Wang PC, Si T, Hsu CC, Wang L, Zayed O, Yu ZP, Zhu YF, Dong J, Tao WA, et al. (2017) MAP kinase cascades regulate the cold response by modulating ICE1 protein stability. *Dev Cell* **43**: 618–629
- Zhou Y, Tan WJ, Xie LJ, Qi H, Yang YC, Huang LP, Lai YX, Tan YF, Zhou DM, Yu LJ, et al. (2020) Polyunsaturated linolenoyl-CoA modulates ERF-VII-mediated hypoxia signaling in Arabidopsis. *J Integr Plant Biol* **62**: 330–348